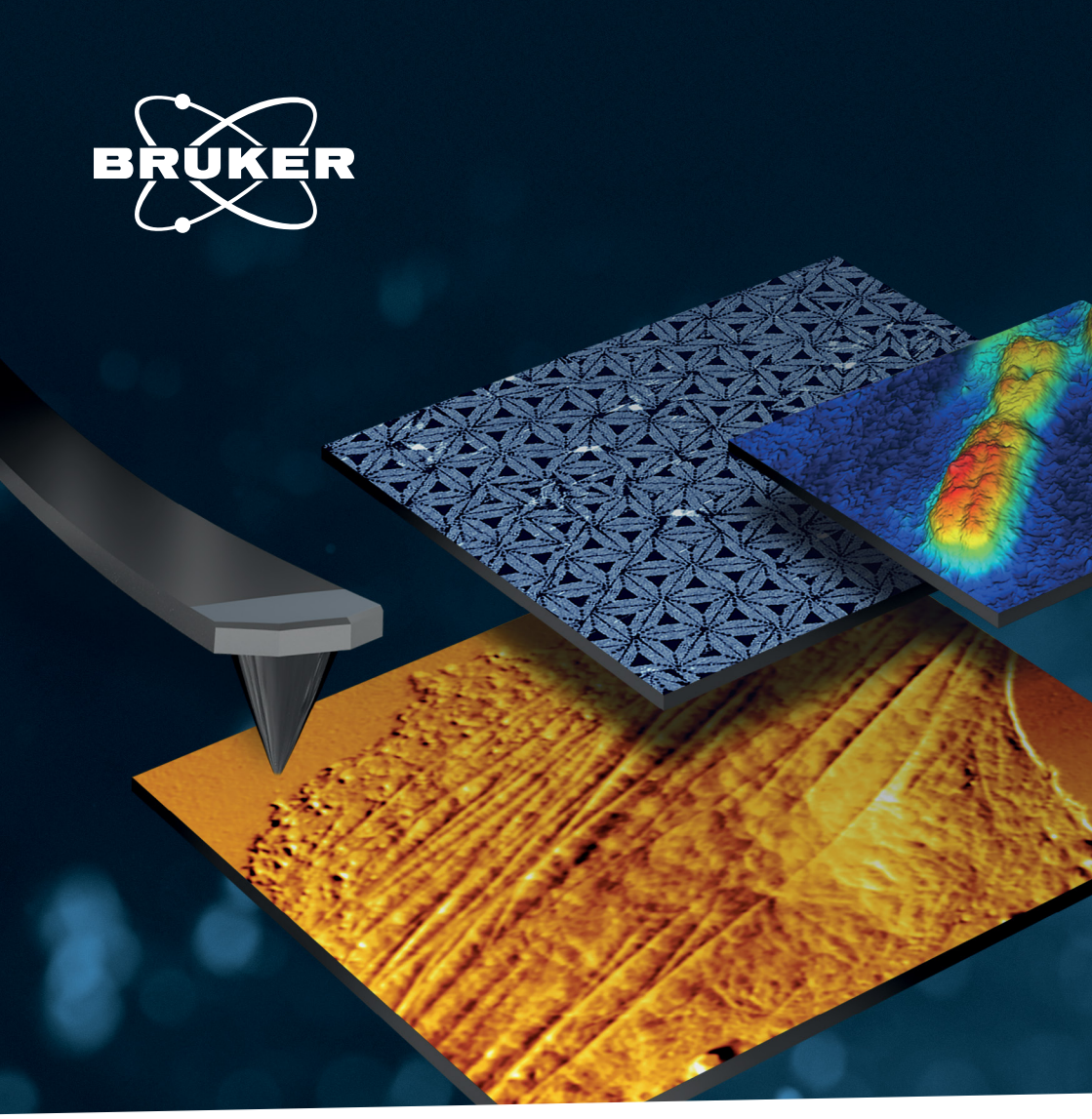

ATOMIC FORCE MICROSCOPY

AFM in the Life Sciences

An Overview

Table of Contents

Foreword

Over the last three decades atomic force microscopy (AFM), a high-resolution surface analysis technique, has become an invaluable research method in labs around the world.

Since its introduction in 1986, the use of AFM in the investigation of biological samples has grown steadily and the technique has gradually developed into a complete toolbox for imaging soft biological samples in liquid. The instruments developed around this technique, commonly referred to as BioAFMs, enable the unique investigation of samples ranging in size from single molecules, viruses, and proteins to living cells and tissues.

Unlike other conventional microscopic techniques, such as fluorescence and electron microscopy, AFM can easily be performed under near-physiological environmental conditions without the need for further sample processing or modification. It enables the real-time, high-resolution visualization of complex biological systems and dynamic processes, as well as the comprehensive characterization of their biomechanical properties.

Furthermore, the ability to easily combine AFM with advanced optical microscopy leverages the advantages of immunolabelling techniques to enable true correlative microscopy.

Introduction

Origins of Microscopy for Biological Sciences

Living cells and tissues are highly organized systems comprised of functional and structural subunits ranging from single molecules to macromolecular structures and organelles that are each vital for life. The fascination for investigating biological matter dates back to the first successful microscopic attempt to observe the cell walls of plant cork by Robert Hooke in 1665 [1]. The first microscopic observation of living cells (*Spirogyra* algae), however, is credited to Antonie van Leeuwenhoek in 1674 [2]. The optical microscope used by van Leeuwenhoek had an approximate two-hundredfold magnification [3]. Since then, various microscopy techniques have been developed that surpass the resolution limit of conventional optical microscopes, revealing continuously greater details in the samples under investigation.

A fundamental leap in microscopy resolution was the invention of the electron microscope in 1930 by Ernst Ruska and Max Knoll [4]. This electron microscope was used by Ladislaus Marton from 1932-1934 to image the first fixed biological specimen, sundew plant leaves [5]. Then, in 1934-35, Eberhard Driest and Heinz-Otto Müller imaged the first biospecimen, the wings and legs of a housefly [6]. Shortly after, Friedrich Krause imaged diatoms, epithelial cells, and bacteria [7, 8].

The principle of both optical and electron microscopy is based on the interaction of either photons or electrons with a sample surface, which, depending on the wavelength used, results in a different resolution. However, in general, neither of these imaging techniques deliver information on quantitative topography of the sample, making them a two-dimensional imaging techniques [9].

The first three-dimensional nanoscale images were acquired in 1982 by Gerd Binnig and Heinrich Rohrer with a technique called *scanning tunneling microscopy* (STM) [10]. In STM, a sharp metal tip

is brought very close to the surface of a sample while an electrical voltage is applied between the tip and the sample, causing electrons to flow between them. This so-called tunnel current is a quantum mechanical effect. By keeping the distance-dependent tunneling current constant while scanning the tip over an area of interest, it is possible to map the topography of the surface at the molecular or even atomic scale. However, to use STM, the sample must be conductive. This is a fundamental limitation for studying biological matter, as the sample needs to be coated with a conductive material in order to be imaged [11]. Nonetheless, STM was used for the first time in 1985 to image biological specimens by Baro et al. [12].

In 1986, the same year in which Binnig and Rohrer were awarded the Nobel Prize in Physics for inventing STM, Binnig and his colleagues replaced the original stiff STM tip with a flexible mechanical cantilever, also known as probe, which led to the invention of atomic force microscopy (AFM) [13]. AFM is based solely on the detection of the interaction forces between the sample surface and a sharp tip attached to the outer end of a flexible lever (mechanical spring), whereby the force-dependent deflection of the lever is measured and quantified (see Figure 1).

The invention of the atomic force microscope not only overcame the resolution limitations of optical microscopes, but also eliminated the need for samples to be conductive. The development of probes with nanometer-sized tip radii and precise XYZ-positioning systems advanced the capabilities of AFMs to enable routine high-resolution, 3D topographic imaging and nanomechanical characterization of biological samples.

Atomic force microscopy has come a long way since its introduction in 1986 [13]. Notable landmarks in the characterization of biological matter include the first image acquired in liquid in 1987 [14], the first observation of a biomolecular process in 1989 [15], the first scientific article on high-speed AFM in 1991 [16], the first high-resolution protein scan in liquid in 1994 [17], the first paper to describe the use of AFM in the study of protein unfolding in 1997 [18], and the measurement of cell-cell adhesion in 2000 [19].

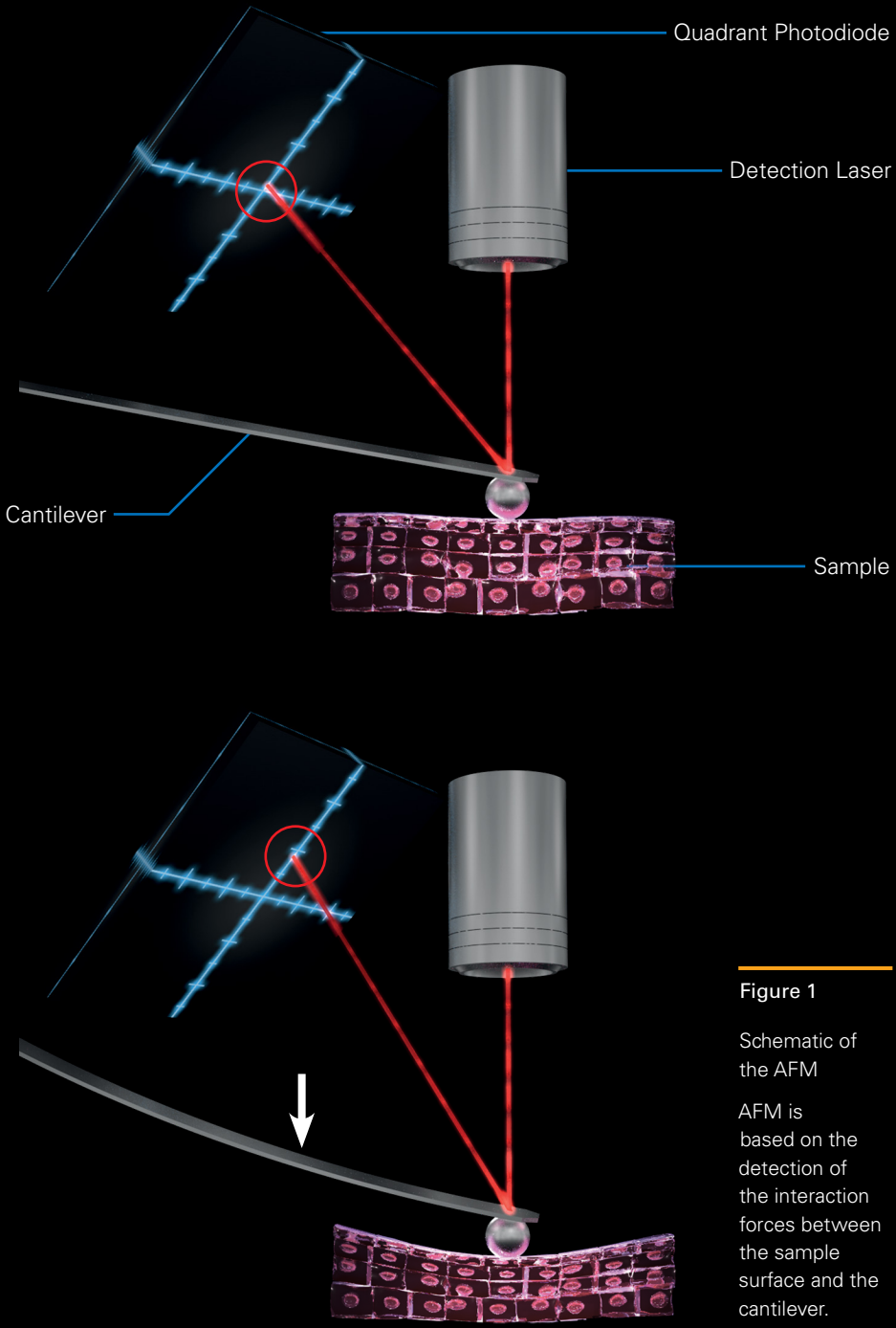

Figure 1

Schematic of the AFM

AFM is based on the detection of the interaction forces between the sample surface and the cantilever.

Comparison of Atomic Force Microscopy with Other Microscopy Techniques

The three most common microscopy methods used in the study of biological matter are optical microscopy, electron microscopy, and atomic force microscopy. The operating principles, imaging conditions, resolution, and sample preparation necessary for each technique differ considerably. A brief overview of the main characteristics and differences is outlined below.

Optical microscopy can be divided into multiple categories, the main ones being bright-field, dark-field, oblique-illumination, fluorescence, phase-contrast, confocal, deconvolution, differential interference-contrast, and dispersion-staining microscopy. Over the past ten years, super-resolution techniques, a sub-category of fluorescence microscopy, have gained particular interest as the resolution of super-resolution microscopy (around 10-20 nm) overcomes the diffraction limit of classical optical microscopy (around 200 nm) [20, 21]. A main advantage of fluorescence labelling is its specificity, which facilitates the highly sensitive identification of specific molecules of interest. However, this mandatory sample treatment, particularly in living systems, is often complex, time-consuming, and, in certain single-molecule scenarios, not feasible without disrupting the function of individual proteins.

Electron microscopy is generally divided into two types: transmission electron microscopy (TEM) and scanning electron microscopy (SEM). Electron microscopy uses an electron beam to create an image, replacing traditional optical lenses with electromagnets. The electron beam interacts with the sample to produce an electron diffraction pattern that is converted into an image. The very short wavelength of the beam enables an approximate thousandfold increase in resolution over classical optical microscopy. In order to be 'visible' to the electron beam, biological samples must be stained or coated with a conductive metal, which results in static snapshots of individual proteins, cells, tissues, and molecular interactions. In addition, electron microscopy operates under vacuum to reduce non-sample related electron scattering, making it impossible to image biological samples under physiological conditions.

Although efforts have been made to develop environmental electron microscopy techniques capable of imaging unstained biological specimens in solution, sample degradation is unavoidable due to the strong electron dose required to achieve high contrast and spatial resolution [22].

While atomic force microscopy was originally invented to visualize atoms on solid interfaces [13], it has gradually evolved into a technique capable of measuring samples of almost any material in any environment. It differs from both optical and electron microscopy in that it does not "see" the sample, instead an AFM "feels" or "probes" the surface. The simplicity of this approach enables the 3D visualization of molecules and living cells in their near native environment.

The use of very sharp tips with optional chemical modifications ensures a resolution on the nanometer scale, high enough to image individual molecules, and comparable to high-resolution electron microscopy. In addition, the use of calibrated probes enables highly accurate force measurements and the comprehensive quantitative characterization of both molecular interactions and the nanomechanical properties of a sample.

AFM is an ideal tool for studying delicate and challenging, living biological samples under near-native conditions. Minimal sample preparation is required and the technique is minimally invasive, allowing direct access to the sample. High-speed imaging capabilities enable the investigation of dynamic cellular and molecular processes [23]. In addition, the ability to combine atomic force microscopy with other microscopy techniques (correlative microscopy) and collect data from the exact same area of the sample, harnesses the advantages of both techniques and delivers complementary data.

Principles of Operation

Basic Working Principle

As mentioned above, atomic force microscopy uses a lever with a sharp tip to sense the surface [24]. To control the horizontal and vertical position of the lever above the surface, piezoelectric actuators are used (that translate a voltage into a length scale) to perform high-precision positioning or movement. One advantage of piezoelectric actuators over other positioning techniques is the resolution that can be archieved (down to the picometre range), which makes high resolution AFM possible in the first place.

As it interacts with the sample, the cantilever bends either towards or away from the sample, a movement that is recorded by a laser beam that is deflected off the back of the cantilever onto a four-quadrant photodetector (Figure 1). The signal measured (voltage) from the detector can be calibrated to reflect the actual spatial deflection of the lever. Assuming that the lever acts like a spring, this spatial deflection can be converted into a force using Hooke's law [25].

In general, the operation of an atomic force microscope can be divided into two basic operating modes, namely AFM force spectroscopy and AFM imaging. In force spectroscopy, the AFM probe approaches a single point on the surface and a so-called force-distance curve is recorded, whereby the deflection of the cantilever is recorded as a function of the distance to the surface (see Figure 2E). In contrast, in AFM imaging, the sample surface is scanned line by line with a sharp probe [24], which is why AFM is also referred to as scanning probe microscopy (SPM).

Commonly Used BioAFM Imaging Modes

Conventional imaging modes use a feedback loop to track the topography of the sample. To do so, the feedback loop requires a distance-dependent reference, or feedback signal, as input. This, for example, can be the deflection of the cantilever which is used

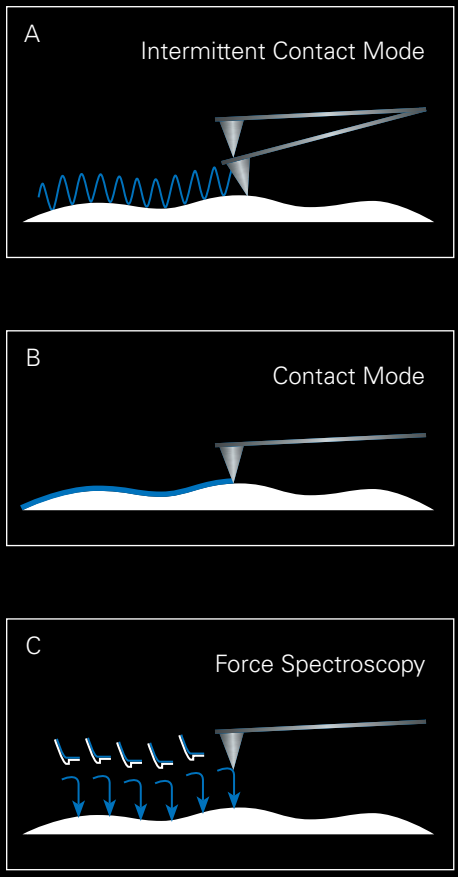

Figure 2

Most common BioAFM imaging modes.

(A) The most frequently used AFM mode is intermittent contact (tapping) mode. Here the cantilever is oscillated at an amplitude close to its resonant frequency and the tip periodically touches the sample surface.

(B) Contact mode (static mode) is used to apply a pre-set cantilever deflection (setpoint) to raster scan the surface without detaching from the substrate.

(C) Force spectroscopy-based modes record complete force curves (vertical application of a pre-set force in an approach/retract regime) at each pixel.

(D) A typical resonance curve of an oscillating cantilever as a function of the excitation frequency. At the resonance frequency, the amplitude (blue) has a maximum value, while the phase (orange) shows a characteristic transition.

(E) Recording and consecutive analysis of a complete force curve unlocks numerous possibilities for extracting both topographical and mechanical information from the sample being analyzed.

to control the distance of the probe above the sample surface by maintaining the feedback signal at a fixed specified value (setpoint). Conventional imaging modes differ depending on the feedback signal used and can be categorized into two main categories: static and dynamic (where the cantilever oscillates) modes.

In addition to conventional imaging modes, new modes have evolved that use a different approach to determine the topography of the surface. This section will provide a brief overview of the most commonly used imaging modes in BioAFM and their application.

The most fundamental AFM imaging mode is contact mode, which is a static mode. Here, the probe is permanently in contact with the sample and its deflection is used as input for the feedback loop which is kept constant (Figure 2B) while the tip moves across the sample. Forces applied to the sample can be accurately quantified during the measurement. However, as the tip is in permanent contact with the surface, relatively high shear forces are exerted on the sample during scanning, which means that contact mode is not generally suitable for delicate biological samples. Contact mode is typically used to study tightly packed, flat macromolecular structures, such as two-dimensional protein crystals and membrane patches.

The lateral shear force that occurs in contact mode can be significantly reduced by using dynamic modes where the probe is oscillated. This is typically achieved by applying a sinusoidal excitation to the base of the cantilever at a frequency close to its resonance frequency. As the oscillation amplitude and resonance frequency of the cantilever exhibit a distance-dependent behavior, caused by the interaction forces with the surface, they can be used as a feedback signal. In particular, dissipative interaction forces affect the damping of the oscillation amplitude, while conservative interaction forces, such as van der Waals and Pauli repulsion, are associated with a shift in the resonance frequency [26].

Amplitude-modulation, also known as tapping or intermittent-contact mode, is the most commonly used dynamic imaging mode in life-

science applications. In this mode, the cantilever is oscillated at a fixed frequency close to its resonance frequency and a constant drive amplitude (see Figure 2A, D). The oscillation amplitude of the cantilever is used as an input signal for the feedback loop. The low lateral forces acting on the sample make the tapping mode ideal for measuring delicate samples. Despite this, measuring the direct force exerted on a sample and interpreting the collected data remains a challenge. In addition, tapping mode can be difficult for beginners to operate and requires a certain degree of AFM experience, in particular when measuring challenging samples and when used in fluids.

TIP

In tapping mode, the force exerted on the sample depends on the amplitude of the free oscillation of the probe. The smaller the amplitude, the lower the forces acting on the sample. However, very small amplitudes are unfavorable as they can increase the lateral forces on the sample or the occurrence of instabilities resulting from adhesion or capillary forces. For this reason, careful tuning is required to find the optimal imaging conditions for a particular sample and environment.

Although both contact mode and tapping mode produce images of excellent quality and are widely used, they are not universally applicable to all biological samples. Each mode has it's own limitations, and beyond measuring topography, neither can characterize the mechanical properties of the sample.

AFM force spectroscopy, on the other hand, can provide insight into the mechanical properties of a sample, such as stiffness, adhesion, etc., at a single point on the sample surface. This is achieved by analyzing the force curve data with physical models, such as contact mechanics models [27]. It is possible to create images from force spectroscopy by recording numerous force curves within a grid across the sample, a process known as force mapping. By analyzing each force curve, it is then possible to determine, for example, the

topography in each pixel of the map. Force mapping, however, is a relatively slow process and can easily take several hours to produce a map with a reasonable number of pixels.

By implementing advanced high-speed electronics and an optimized motion scheme to suppress oscillations of the cantilever, Bruker succeeded in transforming force curve-based mapping into a practical, more universal imaging mode called Quantitative Imaging (QI). QI is a high-speed force measurement technique that captures an entire force curve in every individual pixel of the image and analyzes it in-situ. The jumping motion of the probe significantly reduces lateral forces. In addition, QI keeps the speed of the probe constant during the force curve, which greatly simplifies analysis of the data with physical models [28, 29].

TIP

As a result of the triggered acquisition of force curves, the QI mode no longer requires a classical feedback to generate the image, which makes it an intuitive and easy-to-use imaging mode. QI mode is particularly suitable for performing nanomechanical measurements on challenging biological samples, such as soft, sticky, or highly structured samples, making it ideal for imaging, e.g, living cells and bacteria.

Bruker's proprietary PeakForce Tapping® mode is another example of a newer type of imaging mode that also relies on force-based imaging but uses a different approach to QI. In PeakForce Tapping, the Z-piezo is oscillated in a sinusoidal motion at a fixed amplitude and at a frequency significantly below the resonance frequency of the probe (off-resonant imaging). A force is exerted on the probe at the lower turning point of the oscillation when it touches the surface. This so-called peak-force is measured and used as an input signal for the feedback loop, enabling the probe to follow the topography of the sample [28]. By recording the deflection of the probe and the Z-piezo position, a force curve can be reconstructed for each oscillation cycle. This technique, known as PeakForce QNM®, allows

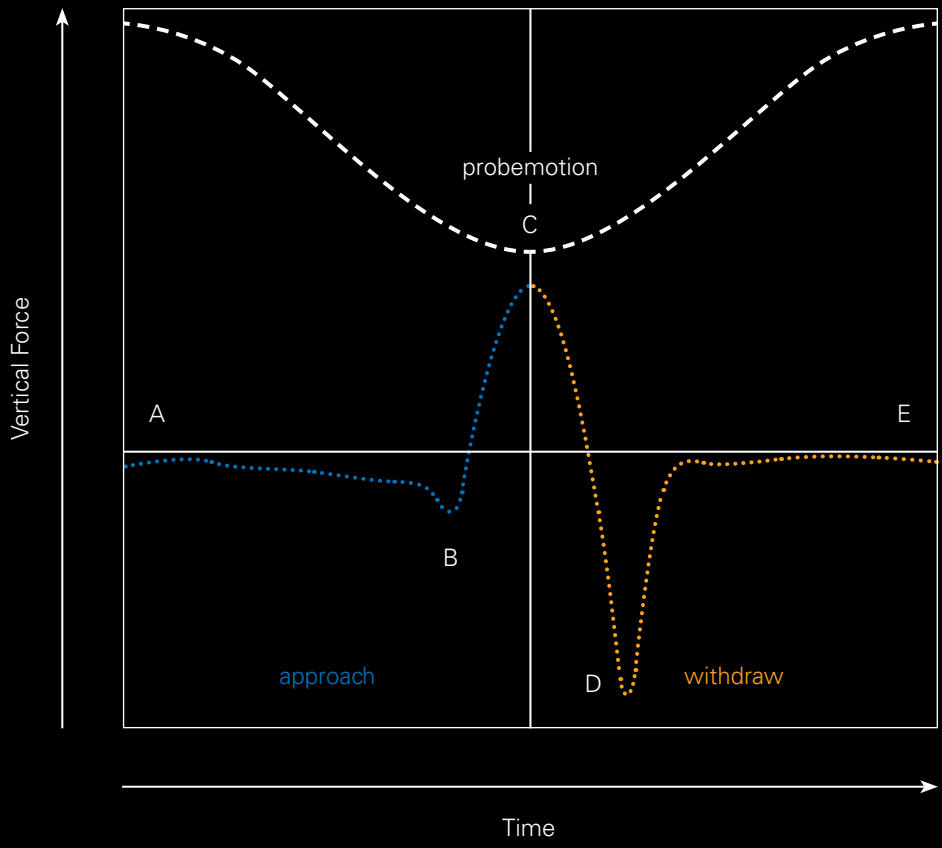

Figure 3

Working principle of PeakForce Tapping.

The cantilever is oscillated in a sinusoidal motion by the Z-piezo of the AFM (dashed white line) well below its resonant frequency. At the lowest point of the oscillation (point C), the interaction with the surface deflects the cantilever. The force exerted on the tip in th is called the peak force and is used to control the distance between tip and sample surface.

the characterization of various surface properties, such as stiffness, adhesion, and deformation, in a single measurement [29].

PeakForce Tapping does not require the cantilever tuning necessary in Tapping mode and is particularly easy to use, even for inexperienced AFM users. Forces exerted on the sample in PeakForce Tapping can be extremely low: down to 10 pN. It is, therefore, particularly suitable for studying fragile or sensitive materials with high resolution. Compared to QI, PeakForce can operate at higher frequencies, which enables faster data acquisition. However, feedback parameters must be taken into consideration and adjusted for.

A significant advancement was achieved with the introduction of Bruker's PeakForce-QI mode, which combines the capabilities of the PeakForce Tapping and QI modes to enable precise, real-time curve monitoring and high-speed nanomechanical imaging of biological samples [30].

Feedback Loop

As mentioned above, many AFM imaging modes use a feedback loop to track the topography of the sample with the AFM tip. Understanding how the feedback loop works is, therefore, essential for achieving the best image quality and optimal surface tracking.

In atomic force microscopy systems, the feedback loop is normally implemented using a proportional-integral-derivative (PID) control loop mechanism. This PID controller is fed with a distance-dependent (feedback) signal, such as the displacement or amplitude of the cantilever oscillation, which is continuously compared with a desired, fixed setpoint. The difference between the two values, referred to as the error signal, is continuously minimized by the PID control loop. As soon as an error signal is detected, the probe is moved accordingly in Z to compensate for the error. The travel distance is determined by a formula that is influenced by three separate control parameters: the proportional (P), integral (I) and differential (D) gain. For simplicity, the differential gain is often ignored in contemporary AFM systems.

Careful adjustment of the P- and I-gains is crucial for accurate tracking of the sample topography. If the gains are too low, the resulting response will be slow and the surface will appear to be blurred. Gains that are too high, on the other hand, can cause the feedback loop to oscillate. As the gains are dependent on the sample stiffness, setpoint, and cantilever resonance frequency, they should be readjusted whenever one of these parameters changes.

TIP

According to the feedback theory, there is an optimum ratio between the I-gain and P-gain. To find this ratio and determine the optimum gains, it is advisable to proceed as follows: First increase the I-gain until the feedback loop starts to oscillate, and then decrease it again until the oscillation stops. Perform the same procedure with the P-gain. Repeat these steps, alternating between the I-gain and P-gain, until it is no longer possible to increase the gains without oscillations occurring.

The image quality is also affected by the imaging speed and applied setpoint. If a sample is scanned too quickly, even the fastest PID control cannot accurately track the topography of the surface. The maximum imaging speed also depends on the height of the sample and, most importantly, the feedback control bandwidth. Similarly, in biological samples, the force applied is typically kept as low as possible. This, however, can ultimately slow down the feedback control.

The feedback bandwidth is influenced by a number of delays inherent in the components of the feedback control system. These include the time required to measure the cantilever oscillation amplitude (in tapping mode), Z-scanner reaction time, and response time of the cantilever [30, 31]. Recent developments that reduce delays in each of these components have been critically important in increasing scanning speeds in high-speed AFM setups.

Instrumentation and Factors to be Considered During Imaging

Cantilever Stiffness and Stylus Geometry

Atomic force microscopy uses a probe that interacts with the surface under investigation. Probes are predominantly manufactured by an etching process and are typically made of either silicon (stiff probes) or silicon nitride (soft probes). Figure 4A shows an SEM image of a standard AFM probe with the tip pointing upward in the center right of the image. The lateral dimensions of the cantilever beam are typically in the micrometer range, while the outer tip radius is usually in the range of 2 to 50 nm. By varying the lateral dimensions and the thickness of the probe, its stiffness can be controlled. However, since the stiffness of the cantilever beam is strongly dependent on its thickness, which is difficult to control accurately in the etching process, the stiffness of commercially available probes can vary widely and must be calibrated in the AFM if forces are to be measured.

The properties of the probe, such as stiffness and tip shape, have an enormous influence on measurements and require careful selection depending on the experiment. Choosing the appropriate probe stiffness can be difficult and may require some trial and error, but there are some general rules. In force spectroscopy experiments, in particular, the stiffness of the probe must match the stiffness of the sample. Using a probe that is too stiff on a soft sample leads to very large indentations that will possibly damage the sample before sufficient deflection of the lever is detected. On the other hand, if the probe is too soft, an adequate indentation into the sample cannot be achieved and it is not possible to derive mechanical information from the data.

In AFM imaging, selection of the probe stiffness depends not only on the sample stiffness, but also on the imaging mode itself. In general, soft samples are imaged with soft probes that gently scan the sample surface without deforming or indenting it. However, it may be necessary to select a stiffer probe when investigating, in particular, sticky samples or working in air where capillary forces occur, to overcome the adhesion of the sample.

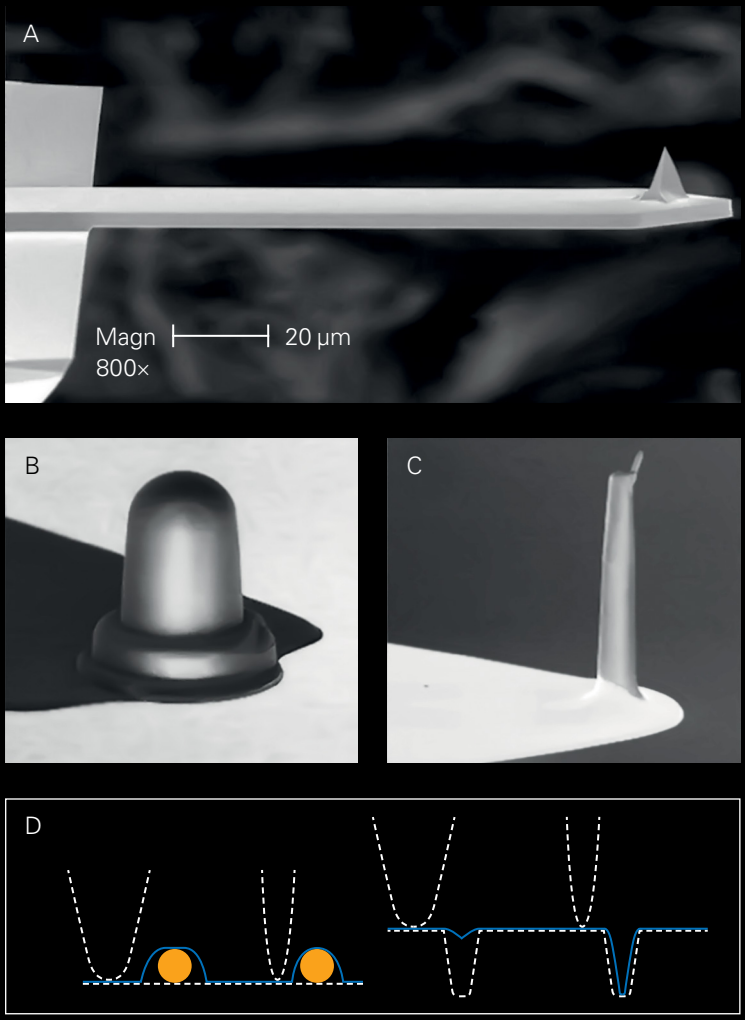

Figure 4

Appearance of different commercial AFM probes and illustration of the tip convolution effect.

(A) Appearance of a standard probe. The actual cantilever is attached to a larger chip (left) and the tip is pointing upwards (center right). (B) Bruker's SAA-SPH probe with a spherical tip for accurate mechanical characterization of soft samples. (C) Bruker's specialized PFQNM-LC-V2 probe combines a high aspect ratio tip with an enlarged tip radius of about 60 nm that is particularly well suited for AFM imaging of living cells. (D) Illustration of the convolution effect between the AFM tip and the surface. The topography acquired with the AFM (blue line) results from a convolution of the AFM tip with the features of the surface.

AFM images are strongly influenced by the geometry of the tip and result from convolution of the AFM tip with the surface features (Figure 4D). The smaller the surface features are compared to the dimensions of the AFM tip, the less accurate the resulting image of the sample will be. When performing high-resolution imaging, such as sub-molecular resolution measurements, it is advantageous to use probes with tips as small as 1-2 nm (radii of curvature). However, although such probes are commercially available, they are comparatively expensive and pick up contamination easily, especially when working in liquids. Furthermore, they can break very easily, leading to unreliable characterization of surface topography and the necessity to frequently change the tip.

When working with living cells, it is advisable to select tips with a larger radius of at least 30 to 60 nm to reduce stress (pressure) between the tip and the cell surface. When measuring tall, highly structured cell surface features, it is also recommended to use tips with a high aspect ratio, the ratio of the height of the tip to its width. Bruker's newly developed PF-QNM-LC-V2 probe (Figure 4C) combines a high aspect ratio with a tip radius of approximately 60 nm, making it the ideal probe for cell surface measurements.

The mechanical characterization of surfaces using AFM force spectroscopy requires a well-defined tip shape or geometry to obtain the most accurate results from the analysis models. Of the various tip shapes available, a spherical shape has proven to be the most reliable for such applications, not least because the pressure on the sample can be controlled by using spheres of different diameters, which is invaluable for the characterization of very soft samples. For these specific applications, Bruker has released a series of probes with spherical shaped tips (Figure 4B) and different diameters.

TIP

During imaging, particularly in liquid, tips can become contaminated, go blunt, develop a "double" tip, or take on an asymmetric shape, rendering these measurements unreliable. When this happens, the AFM tip should be replaced immediately. Although it is possible to clean a cantilever - numerous cleaning protocols are available - after cleaning, it is necessary to ensure that the shape and size of the cleaned tips are still intact using an AFM calibration grid. These measurements are very time-consuming and, in most cases, only confirm that the tip cannot be reused.

Tip-Sample Interactions and Sample Deformation

When an AFM tip touches the surface of a sample, both the tip and sample are subject to deformation. The larger the force applied to the sample, the greater the deformation, which in turn is related to the size of the tip-sample contact area [32]. For this reason, it is important to keep both the contact area and the forces acting on the sample as low as possible to achieve the best possible resolution. However, a certain minimum force must be exerted on the sample to achieve the best possible contrast of the structures being imaged.

TIP

To achieve sub-molecular resolution on protein samples or DNA/RNA, it is advisable to maintain forces at around 50-100 pN during the measurements. Forces in this range provide the best balance between the tip-sample contact area and the minimum force required to distinguish between sub-molecular features.

To visualize the internal structure of living cells, such as the cell body, cell membrane, cytoskeleton, or nucleus, it is necessary to apply sufficient pressure on the cell to significantly indent the surface. This can be achieved by applying higher forces in the range of 300-500 pN. Even at lower forces, the resulting images of soft living cells do not reflect the true topography of the cell surface, as it is not completely possible to prevent the tip from indenting the surface. The actual surface topography can be determined using contact point imaging, which is derived from force curve-based imaging modes, such as QI or PeakForce QNM. The contact point, i.e., the point where the tip just touches the surface and the applied force is almost zero (see Figure 2E), can be taken directly from the force curves and displayed as an image [33, 34].

Optimizing BioAFM Design for Use in Life Science Applications

The scope of samples that can be studied with BioAFM and the range of applications are very diverse, spanning from the imaging of single molecules to the visualization of molecular interactions, biomechanical characterization of living cells and tissues, and preclinical research. For this reason, many factors must be taken into consideration when choosing an AFM technique or mode for a particular application. These include the sample environment (fluid/air), imaging speed, handling flexibility, and the option to integrate with optical microscopy techniques.

Combining AFM with Advanced Optical Microscopy

While AFM offers excellent resolution and direct access to the sample, it lacks the ability to chemically characterize surface features and the scanning area is limited (typically to 100 × 100 µm²). These limitations can be overcome by combining AFM with advanced optical techniques, such as fluorescence microscopy.

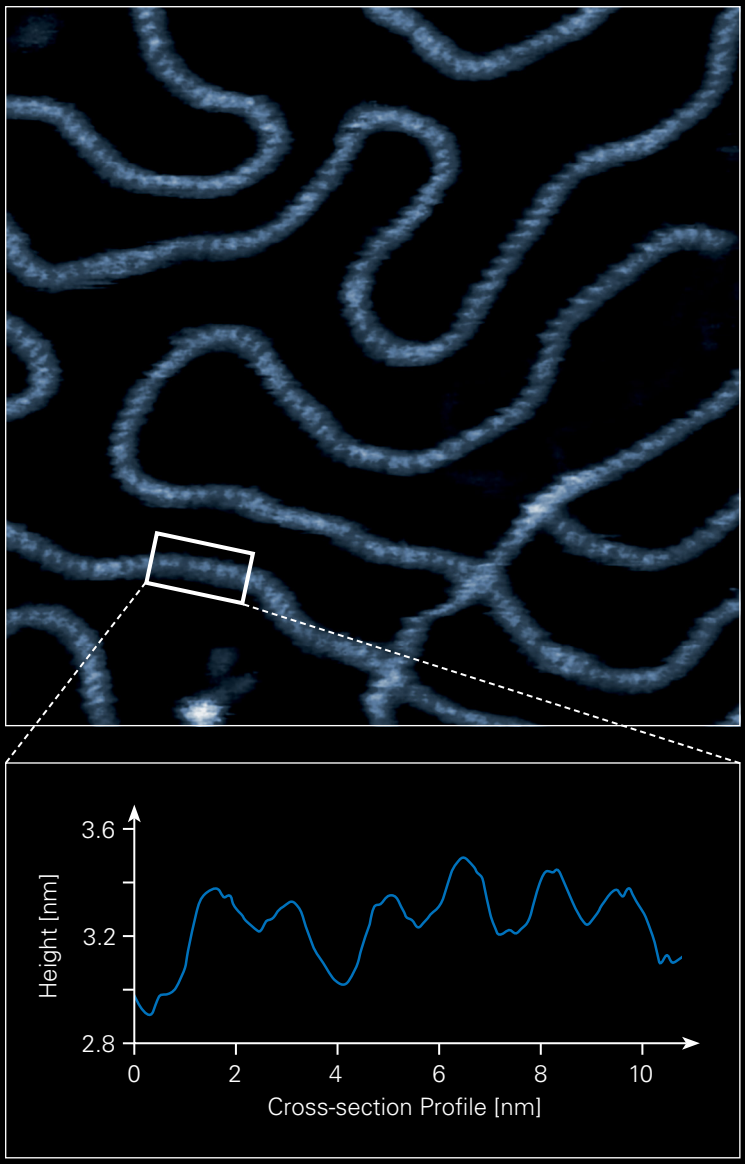

Figure 5

High-resolution image of puC19 DNA showing major-minor groove resolution (inset).

Image acquired using tapping mode in liquid and a Bruker FASTSCAN-D probe.
(Scan size: 87.5 nm × 87.5 nm, height range: 3.5 nm)

Fluorescence-based optical techniques, in particular, allow the identification of specific biomolecules, cellular structures, organelles, or antigens via specific fluorescent labelling. The larger field of view provided by optical techniques enables the identification of areas of interest that can then be analyzed by the AFM. For this reason, the combination of AFM with an advanced optical microscope is now standard when imaging biological samples, as it delivers complementary datasets and correlated measurements.

When choosing an AFM for correlative measurements, various factors need to be taken into consideration, such as the type of scanner and the optical design of the AFM head. In general, atomic force microscopes are classified as either tip-scanners, in which the AFM probe is scanned over a stationary sample, or as sample-scanners, in which the sample is actively scanned under a stationary AFM probe. In BioAFM, the tip-scanning configuration provides significant advantages with regards to system versatility and sample size. As the sample is stationary, tip-scanning systems can accommodate much larger, heavier samples and are more easily modified to enable integration with other techniques. The tip-scanning design is also advantageous for applications where the optical image of the sample needs to remain in focus during the AFM measurement. This enables the simultaneous, timelapse collection of both AFM and optical data [35, 36]. In theory, this can also be achieved using a sample scanning setup, the workflow, however, is considerably more complicated, involving either interlaced scanning (consecutive line-by-line acquisition with each technique), imaging by each method one after another, or correlated movement of both the sample and optical microscope lenses during imaging. Each of these approaches, however, can lead to adverse effects such as thermal drift, mechanical noise, or vibration, which are particularly disruptive when studying dynamic biological processes or sensitive molecules, and should be avoided at all costs.

When combining AFM and optical data, the different physical sizes of the images and non-linear distortions, such as lense aberrations, must be taken into consideration. Recent advances in imaging techniques and software have reduced the gap in resolution

Figure 6

A NanoWizard AFM integrated with an inverted optical microscope.

between AFMs and optical microscopes [37-40], enabling users to overlay and compare datasets from the two techniques. One such advance is Bruker's DirectOverlay feature, a patented calibration method that achieves perfect optical integration by precisely correlating AFM and data from various optical techniques [41]. DirectOverlay utilizes the accuracy of a modern AFM scanner to correct for the imperfections associated with optical images, such as spherical aberrations, by means of a calibration process [42, 43]. Using DirectOverlay, advanced optical microscopy data can be perfectly overlaid in the same viewing window as atomic force microscopy data and viewed simultaneously. It can be used with a wide range of advanced optical techniques, including confocal microscopy, stimulated emission depletion (STED) microscopy, structural illumination microscopy (SIM), and stochastic optical reconstruction microscopy (STORM), etc. [44].

Enabling the Investigation of Molecular & Cellular Dynamics

When studying molecular and cellular dynamics, it is crucial to consider the timescales of the biological processes involved. Events such as cellular translocation, membrane vesiculation, cytoskeletal dynamics, protein fibrillogenesis, or DNA kinetics occur on the timescale of seconds and milliseconds. This requires tools capable of both high spatial and temporal resolution. Over the past 15 years, impressive advances have been made in the availability of ultra-small cantilevers and AFM components, such as piezo actuator-based sample scanners and optical beam deflection (OBD) detectors. These tools have enabled the study of high-speed single-molecule processes [45-47], but their small scan ranges of only a few micrometers in XY and less than a micrometer in Z generally prevent them from being used to study living cells [48, 49]. Recent advances in fast, tip-scanning AFMs have, however, facilitated the structural analysis of various dynamic cellular processes, such as exocytosis, vesicle transport, cytoskeleton reorganization, and cell migration, which occur on the timescale of seconds and milliseconds [34, 50]. The ability to resolve cellular events and structural changes in the surface morphology is no longer fundamentally limited by the conventional optical diffraction limit, and here too, combining an AFM/BioAFM with optical/fluorescence detection systems is advantageous [51].

Innovative Solutions for Larger Sample Areas – Studying Tissue and Multilayer Cell Systems

Until recently, conventional AFMs could only be used to characterize the nanomechanical properties of single molecules, cells, and thin tissue sections [27]. However, the requirement to study larger biological and clinical samples that are often inhomogeneous, rough, and difficult to modify in their native state, has led to a host of advances in AFM instrumentation [52].

Conventional AFM scanners are generally restricted to an XY scan range of 100 µm × 100 µm and 15 µm in the Z direction. While this configuration keeps the inherent positional noise of the piezoelectric scanner to a minimum, thereby enabling high-precision imaging and spectroscopy measurements, it is not suitable for studying larger samples such as biomaterials, implants, and model organisms in developmental biology (zebrafish, C. elegans, etc.). To cope with the larger lateral dimensions of such samples, motorized stages have been introduced that can effectively extend the XY scan range of the AFM to several millimeters, by, for example, using a software tiling feature which collects several scans or images over a larger area and then combines them to form one large composite image.

The larger samples mentioned above, however, typically exhibit large variations in height that exceed the Z scan range of a typical AFM. For this exact purpose, Bruker has developed the HybridStage, a stage that enables the mechanical characterization of such samples. It combines a motorized stage with an integrated piezo-based XYZ sample scanner and provides an optional scanning range of up to 300 µm [53, 54]. The HybridStage is primarily designed for force spectroscopy applications and enables the comprehensive nanomechanical characterization of most of the challenging samples mentioned above [52, 55].

The Bruker software feature SmartMapping offers an alternative approach for the mechanical characterization of rough samples [56].

SmartMapping is based on force mapping and uses the AFM's integrated Z-motors to virtually extend the limited Z-range of the AFM's Z-piezo. This is achieved by adjusting the motors in Z and recording the corresponding distance as soon as a force curve leaves the Z-piezo range. Unlike traditional mapping, where a map is always rectangular in shape, SmartMapping allows the free-hand selection of user-defined shapes and areas for the 2D force maps. In this way, only specific areas of interest on the surface are mapped, dramatically reducing the acquisition time.

In order for atomic force microscopy to perform high-speed measurements, specialized hardware is required [57, 58]. Fast feedback, in particular, can only be technically achieved by using Z-scanners with a small stroke, typically below 2 µm. This, however, makes high-speed AFM unsuitable for the investigation of highly corrugated samples such as living cells, bacteria, or tissue samples. To address this issue, several solutions have, in the past, been suggested, e.g., the combination of different scanner types [59-61], innovative feedback loop architectures, and various combinations of tip and sample Z actuators [62, 63].

Bruker's NestedScanner technology is a commercial solution specifically developed to overcome the limited Z-range in high-speed applications [64]. It uses two Z-piezo actuators simultaneously: an internal head piezo (up to 15 µm) and the piezo of an additional, high-resonance frequency fast-scan cantilever holder (up to 1.5 µm). This two-phase actuation increases the scan rate without reducing the Z-range of the AFM or limiting the height of the sample. Furthermore, this dual-actuator combination can be applied in force spectroscopy to speed up the acquisition process [65]. This is particularly useful when using large, slow scanners (100 µm).

Environmental Solutions and Add-Ons

In general, the investigation of biological samples necessitates working under near-native conditions, i.e., in a liquid environment with the appropriate buffer composition, salinity, pH, etc. Additional requirements include the ability to control the temperature or accommodate various substrates and samples. The wide variety of requirements cannot be met by one universal environmental control option, which is why it is important that a BioAFM offers a selection of add-ons that allow a broad range of AFM experiments on a diverse range of biological samples. Bruker offers an extensive range of environmental add-ons, such as biocells and fluid cells.

The most commonly used sample-supports in biology are coverslips, glass slides, and Petri dishes. They can all be used with AFM, and as they are transparent, they allow the combination of AFM with advanced inverted optics. Petri dishes are ideal for the cultivation and immobilization of cells and are often used for the investigation of living cells with AFM. Bruker has developed the PetriDishHeater (Figure 7A) that accommodates a wide range of commercially available 35 mm dishes, allows active heating of the sample at up to 60 °C, and gas exchange to keep CO_2 saturation at a defined level, enabling long-term studies on living cells.

In addition to Petri dishes, which are typically made of plastic, glass coverslips are also widely used in AFM measurements. Not only can the surface of the glass be easily modified to allow sample immobilization or functionalization, but the thinness of coverslips (130-170 µm) makes them ideal for combining AFM with high-resolution inverted optics. Coverslips, however, are sensitive to mechanical vibrations that can negatively affect an AFM measurement, resulting in unwanted background noise. Bruker's BioCell (Figure 7B) has been specifically developed to counteract the effect of unwanted mechanical vibrations. It is a liquid cell that can be actively heated and cooled within the range of 15 °C to 60 °C and is equipped with capillary ports. If mechanical vibrations are less critical in an experiment, thin glass-bottomed Petri dishes can be used as an alternative, as they offer a wider field of view and larger sample volumes.

TIP

To accommodate the widest range of possible applications, liquid cells should be equipped with capillary inlets and outlets. These ports allow buffer exchange or the introduction of proteins or analytes that can trigger or influence the course of a measurement. The perfusion and exchange of fluids and gases is often essential, in particular when studying living cells or the dynamics of biological molecules in-situ.

A wide range of temperature control solutions are available that enable experiments to run in a temperature range of -120 °C to +80 °C (in liquid) or up to +300 °C (ambient conditions), which is useful for studying samples such as polymers.

When working with biological samples, the safety of staff and the environment is of utmost importance. Any component, cantilever holder, or membrane, etc. that is exposed to a sample must be clean and, if necessary, sterile. Therefore, all components that come into contact with a sample should be easy to disassemble and clean, either by rinsing, ultrasonication, or standard sterilization protocols. This is particularly important when working with pathogens in biosafety facilities. Bruker BioAFMs and add-ons are designed with this requirement in mind.

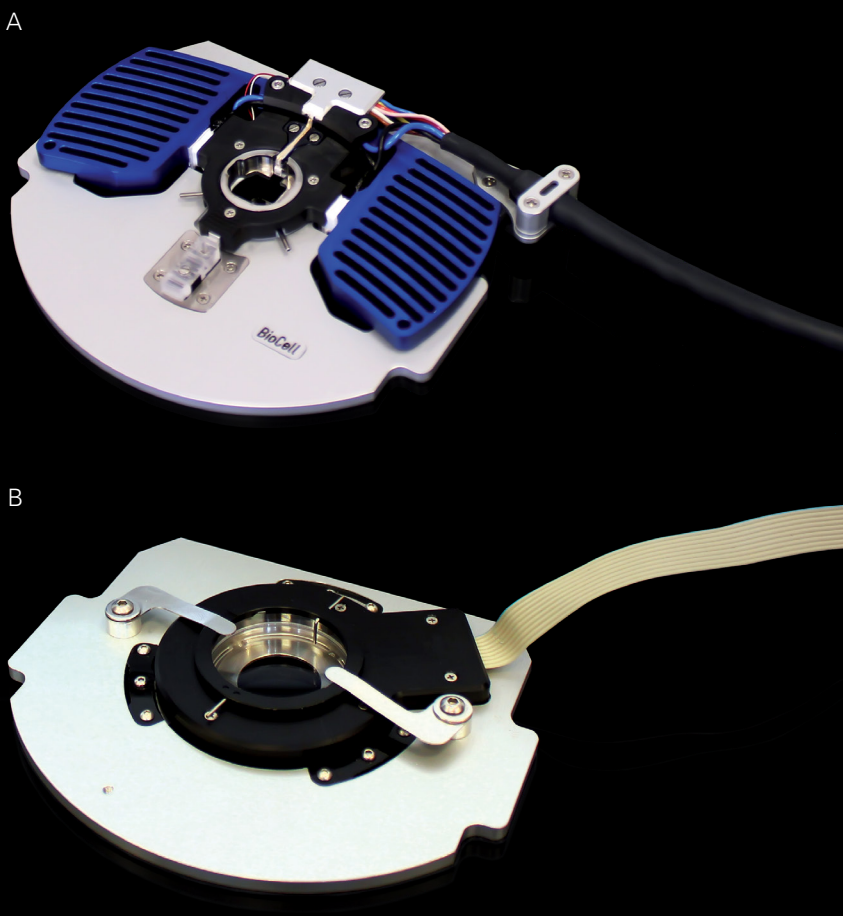

Figure 7

Common fluid cells offered by Bruker for biological applications with the AFM.

(A) The PetriDishHeater accommodates many commercially available 35 mm Petri dishes and provides temperature control. It is commonly used for live cell experiments with AFM. The capillary tubes attached can be used to control CO2 exposure.

(B) The BioCell accommodates thin glass coverslips and enables the combination of high-resolution inverted optics with AFM. It has been specifically optimized to suppress the mechanical vibrations that can occur when using thin glass coverslips, and enables active heating and cooling of the sample. Built-in capillary tubes allow the exchange of liquids and gases.

Case Studies and Applications

The ability of BioAFMs to perform high-resolution imaging, characterize nanomechanical properties under near-physiological conditions, and integrate with advanced optical microscopes has resulted in the growing recognition of atomic force microscopy in life science research. Its use has extended into related fields, such as biomedical research, diagnostics, tissue engineering and many more. In addition, recent developments in high-speed AFM have also made it possible to explore dynamic processes.

This section will provide an overview of the latest innovative applications for BioAFM and demonstrate its potential across a diverse range of fields.

DNA Imaging and DNA-Based Nanotechnology

Deoxyribonucleic acid (DNA) is currently one of the most intensely used biological molecules in nanotechnological applications. Its inherent structure features two alpha-helical strands that have four different nitrogenous organic bases deposited along a central sugar-phosphate backbone, giving the double helix unique binding properties. The orientation of the nucleobases ensures that they only interact with each other in accordance with the complementarity code (pairing rules) and twist around the central axis in a way that minimizes contact of the hydrophobic sugar-phosphate backbone of the DNA with water. This ultimately results in a right-handed, double-helical structure with a characteristic 3.4 nm repeat comprised of a major and a minor groove (2.2 nm and 1.2 nm). DNA molecules can be routinely imaged in liquid with a BioAFM, as seen in the example of a plasmid DNA (pUC19) deposited on a poly-l-ornithine substrate (Figure 8A). DNA, both in vivo and in vitro, often exists in so-called supercoiled states that are high in torsional energy [50], often driving the transient dehybridization of the double-helical regions of DNA. This high-resolution image of the double-helical structure of DNA demonstrates how BioAFM can be used to study fundamental DNA and RNA-based processes in molecular and cellular biology, such as

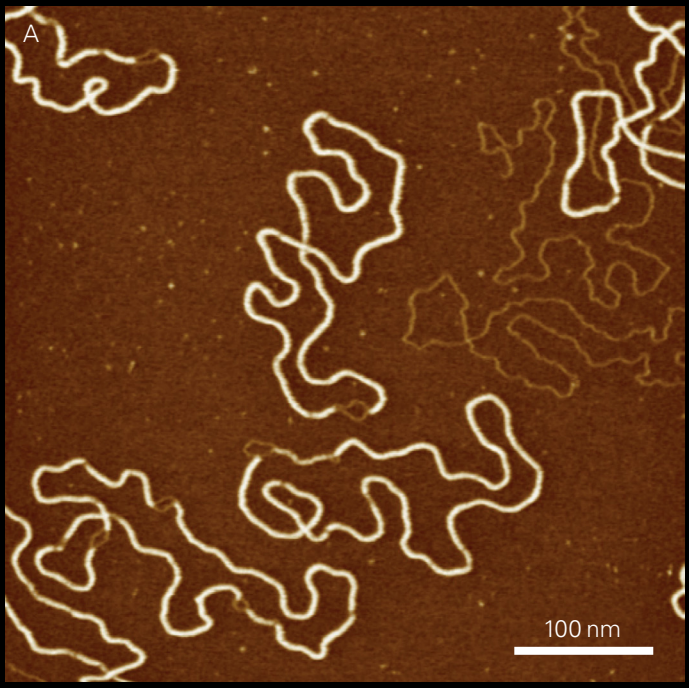

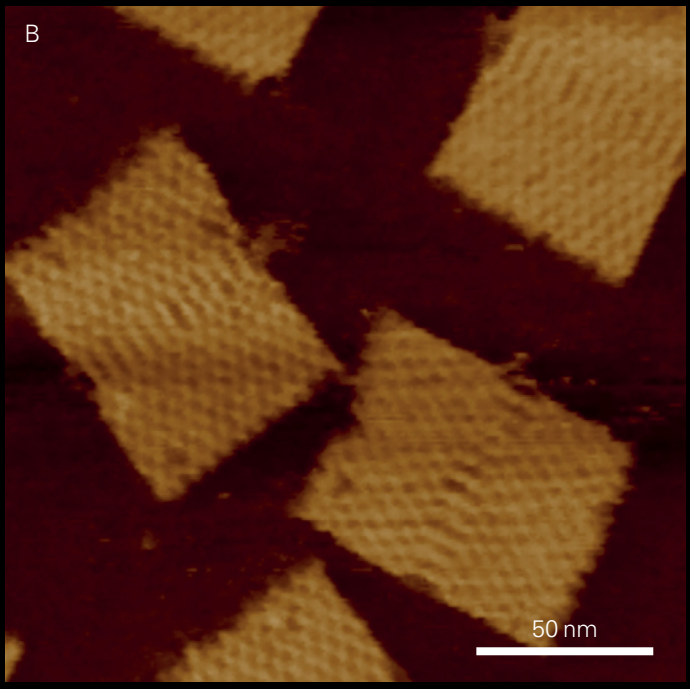

Figure 8

BioAFM Images of DNA molecules and DNA origamis.

(A) Topography of pUC19 plasmid DNA strands. Certain locations along the DNA strands show partial dehybridization of the double helix, as an attemptto minimize the torsional energy of the super-coiled constructs.

(B) Height of a GATTA-AFM DNA origami lattice recorded in liquid. The partially visible gaps in the origami template are introduced via shortened staple strands in the origami design and serve as binding handles for additional molecular functionalities.

transcription, replication, recombination, repair, and even polymerase chain reaction (PCR).

DNA origami nanotechnology has become increasingly popular since the introduction of DNA origami designs in 2006 [66], and has promising applications in biomedical engineering, diagnostics, and therapeutic development [67]. It features the complementarity, base-pairing encoded design of well-defined scaffolds, and recent advances have shown excellent control of the 3D shape and function with nanometer accuracy [68]. DNA origami enables fast prototyping and precise engineering of molecular geometry, mechanics, and dynamics [69].

Figure 8B shows a rectangular origami template imaged using tapping mode AFM. The planar structure of the 100 nm × 70 nm origami is created from a linear single-stranded DNA with multiple, short, complementary single-stranded staples. Currently, such structures and many more can be conveniently designed using software that enables the creation of 2D and 3D origami designs with a myriad of structures and binding functionalities [70, 71].

DNA Origami Nanostructure Dynamics

DNA origami nanostructures (DONs) have emerged as excellent molecular pegboards for the immobilization of ligands onto surfaces, allowing the study of receptor stimulation and early signaling events in adherent cells [72]. The bottom-up self-assembly of such supramolecular architectures can be exploited to create bio-instructive materials, such as nanocomposites for cell receptor stimulation [73] or biosensor surfaces for investigating nanoscale effects on early cell signaling events [74]. These kinds of applications take advantage of the effective linkage between receptor ligands and the DONs via high-affinity biotin-streptavidin bridges.

Figure 9 shows an example of this type of structure bearing five biotin binding sites in the presence of streptavidin and imaged with BioAFM in liquid. This scenario could encompass any molecule of interest (growth factors, enzymes, etc.) that carries a corresponding

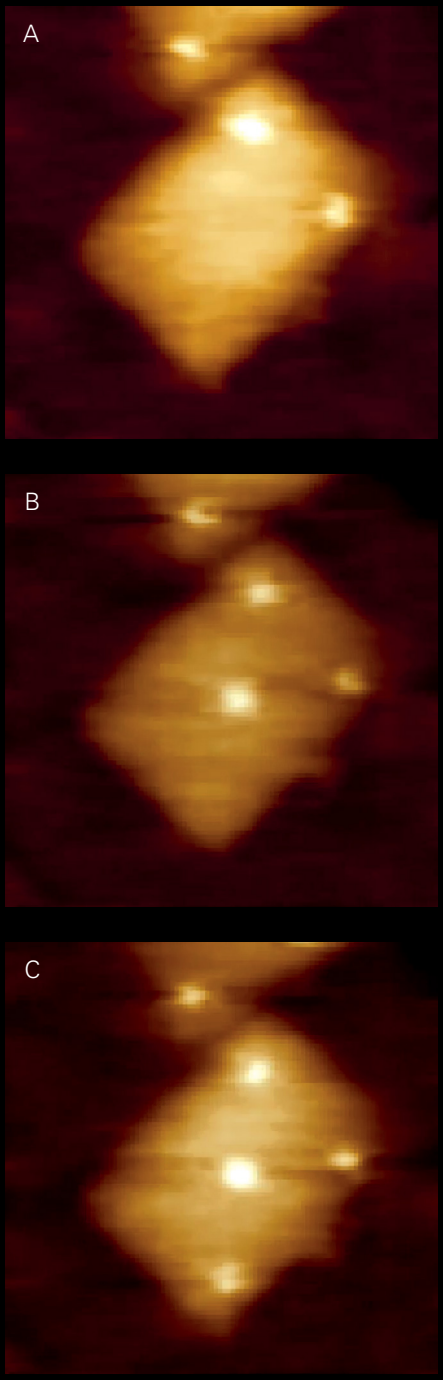

Figure 9

DNA origami nanostructures carrying 5 biotinylated binding sites.

The topography images show consecutive binding of streptavidin molecules to the binding sites carrying biotin tags.

The bright dots appearing in A, B and C designate 2, 3 and 4 biotin-streptavidin complexes on the lattice surface.

The snapshots are part of a longer video sequence (1,407 frames), recorded with a high-speed BioAFM at an acquisition rate of 50 frames/sec.

The full video sequence can be found here:

youtube.com/watch?v=2QTnGQ9JmZI

tag and can be influenced in a concentration-dependent manner. Here, to visualize the kinetics of streptavidin-biotin binding, a mica substrate was initially loaded with biotinylated DONs and then injected with streptavidin. To visualize the dynamics, high-speed imaging was performed at an acquisition rate of 50 frames/sec. The selected images demonstrate the consecutive occupation of the biotinylated binding sites with streptavidin molecules. By quantifying the occupancy of the binding sites over time, conclusions can be drawn about the binding properties, in particular, the binding strength [49].

The use of DNA origami nanostructures is an excellent way of investigating cell culture systems, as various molecular components, proteins, and nanoparticles can be used as signaling cues, making the techniques a valuable asset in life science research.

AFM-Based Single-Molecule Force Spectroscopy

Understanding the forces that govern specific molecular interactions can be challenging in structural biology due to the diversity of interactions and bonds that form between individual molecules [75]. AFM-based single-molecule force spectroscopy (AFM-SMFS) is an experimental methodology that enables the study and manipulation of the mechanical properties of individual molecules [76]. Intermolecular interactions are an integral element in, for example, receptor-ligand binding, cell signaling, protein-complex formation, antigen-antibody interactions during an immune response, and in single molecule interactions in macromolecular complexes. AAFM-SMFS can also be used to study intramolecular interactions in multi-domain proteins, DNA, and polysaccharides.

Studying intramolecular forces with AFM-SMFS has provided invaluable insights into biomechanical properties, folding pathways, kinetics, and the functional properties of biological molecules in both healthy and diseased states, opening the way for AFM-SMFS as a diagnostic tool in pathogenesis.

To study the intramolecular forces involved in protein unfolding, the molecules of interest must be held between the cantilever tip and the sample surface. This is typically achieved by either non-specific physisorption interaction forces between the sample (molecule) and the tip (e.g., via an electrostatically charged tip), or by attaching specific molecules to the tip via functionalization with an immunochemical method. The attachment of an extension linker or spacer to either the tip, sample, or both can help reduce unwanted interactions and prevent the direct attachment of single molecules to either the tip or substrate surface [77]. It is also possible to use recombinant or artificial multi-domain polyproteins, in which certain domains or structures have been co-expressed, allowing the structural analysis of specific protein domains or sub-domains [78] or the characterization of the mechanical properties of novel elastomeric proteins [79].

Figure 10 shows the unfolding of individual (GB1)8 polyproteins. Each molecule is the result of a recombinant protein expression and constitutes eight full copies of the GB1 (guanine-nucleotide binding protein) molecule (Figure 10A). This molecule has attracted a lot of interest recently because of its superior mechanical properties that are comparable to elastomeric proteins in vivo. Furthermore, it shows a unique combination of mechanical properties: fast folding kinetics, high folding fidelity, and low mechanical fatigue during repeated stress-relaxation cycles.

A typical unfolding force-distance (FD) curve of polyproteins like (GB1)8 shows a saw-tooth pattern with up to 8 events that result from the complete unfolding of each GB1 subunit (Figure 10B). At low tension (applied forces), the individual molecular chains of the polyprotein can be straightened in a process of entropic elasticity, also referred to as thermal unbending [80, 81].

At this level, the freely jointed chain (FJC) and worm-like chain (WLC) models are used to describe the process and extract parameters that describe the individual unfolded domains, such as contour and persistence length. Figure 10B shows how the WLC model can be applied to fit the FD curves and extract the contour length of each unfolded GB1 subunit.

Fully automated SMFS enables the acquisition of thousands of FD curves, which is advantageous for statistical purposes and ensures reliable data (Figure 10C). Bruker's ForceRobot® 400 currently achieves 250,000 FD curves per day, delivering statistically relevant, precise measurement of multiple characteristic parameters, such as the average unfolding force (173 pN) of an individual GB1 domain and the mean contour length (19.2 nm) of a fully unfolded GB1 amino acid sequence (Figure 10D).

Multiparametric Imaging of Living Cells

Traditional AFM modes, in particular contact mode, face challenges when imaging complex biological samples that have steep edges, are soft and sticky by nature, or are loosely attached to the substrate. These challenges can be partially addressed using tapping mode and hardware modifications, but these require a certain degree of expertise and preliminary knowledge about the dimensions of the specimen.

Commercially available fast force-mapping modes and algorithms (e.g., Bruker's QI) that were specifically designed to characterize challenging biological samples are better suited. Instead of tracing the surface of the sample, the cantilever records a force curve at each pixel of the image reducing the lateral forces typical in contact mode to a minimum. Lateral movement between pixels only occurs once the cantilever has fully detached from the substrate.

Figure 11 shows an example of multiparametric, correlated imaging performed on living murine NIH-3T3 fibroblasts using PeakForce-QI. The cells were fluorescently stained (Figure 11A) and kept in Dulbecco's Modified Eagle Medium (DMEM) at 37 °C.

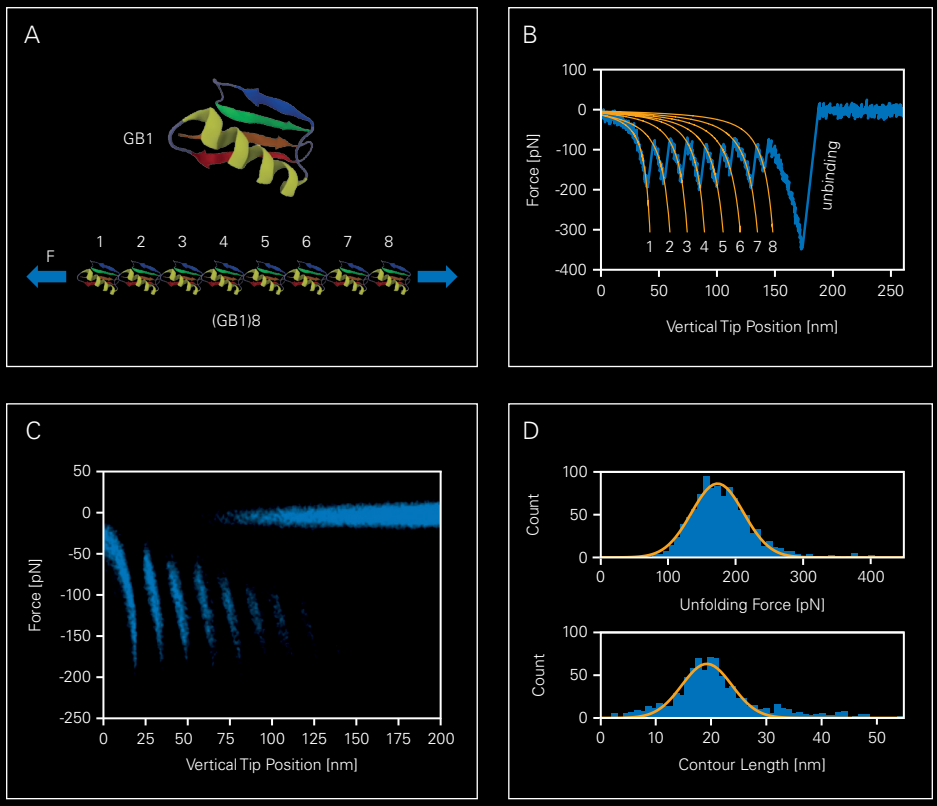

Figure 10

AFM-SMFS unfolding of (GB1)8 polyprotein.

(A) 3D render of an individual GB1 and the corresponding recombinant polyprotein consisting of eight tandem repeats of GB1. "2J52" structure from the RCSB Protein Data Bank was used to display the GB1.

(B) Characteristic force distance (FD) curve demonstrating the complete unfolding of all subunits in the polyprotein. The contour length of each unfolded GB1 subunit was determined by fitting the FD curves with a worm-like chain model (red).

(C) Density plot of superimposed FD curves indicating the probability of unfolding up to 8 subunits.

(D) Distribution of contour length and unfolding force values for GB1 subunits. Mean contour length determined is 19.2 nm, with an average unfolding force applied of 173 pN.
Sample courtesy of Prof. Yi Cao, Dept. of Physics, Nanjing University, China.

Recording a complete force curve at every pixel enabled the complete tomographic reconstruction of the cell surface within the applied force range of 0 to 300 pN (Figure 11B).

By applying a contact mechanics model, it is possible to calculate the Young's modulus (the ratio of stress to strain within the elastic limit) of the sample (Figure 11C). By recording a complete FD curve, it is possible to differentiate between the information obtained at each level within the cell during indentation (Figure 11D). This enables the visualization of specific structures, such as the cytoskeletal F-actin which becomes visible at 300 pN (Figure 11E) and the cell surface membrane which becomes visible close to 0 pN (Figure 11F). This data is accessible during both the in-situ measurements and off-line for more advanced data analysis.

Dynamic Mechanical Analysis of Soft Materials

Living cells and tissues are complex materials composed of different structures and compartments that continuously regenerate and remodel. Traditionally, the mechanical properties of such systems were primarily analyzed using classical Hertzian mechanics models that provide invaluable insight into their apparent stiffness [27]. However, in the case of living cells and tissues, the mandatory Hertzian assumptions of isotropic linearly elastic materials do not apply as a result of their complex inhomogeneous composition and interactions with their surrounding environment [82]. It has become increasingly apparent that an advanced analysis of biological systems requires models that go beyond pure elasticity [83-86].

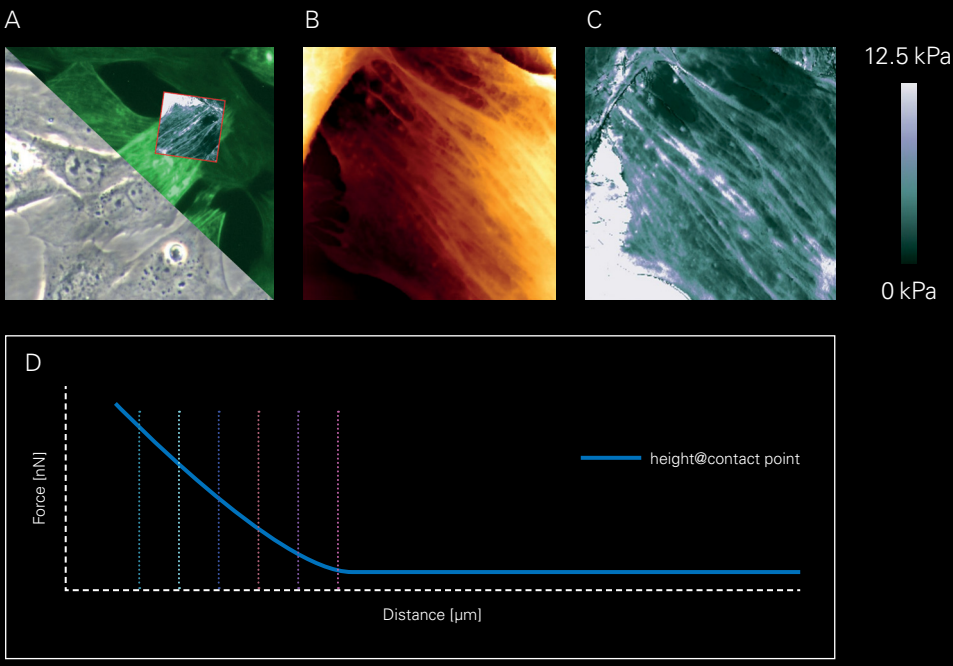

Figure 11

Multiparametric Imaging of Living NIH-3T3 Fibroblasts

(A) Phase contrast (lower left) and fluorescence (CellMask™ Plasma Membrane Stains (thermofisher.com) green actin tracking stain) images (upper right) of living murine fibroblasts measured in cell medium at 37°C. PeakForce-QI measurements were performed in the inset region in (A) to record the setpoint topography (B) and determine Young's modulus of the cell region (C). The collection of complete force curves at each pixel enables accurate determination of the contact point and tomographic reconstruction of the cell surface/height at different reference forces (D). The corresponding cell surface images at 300 pN (E) and near 0 pN (contact point imaging, F).

Figure 12A shows a characteristic FD curve recorded on living cells. The hysteresis observed between the approach and retract segments occurs as a result of the viscous response of the sample. In addition, by applying oscillations in the Z direction while the cantilever is in contact with the sample, it is possible to measure the frequency-dependent response of the material. The indentation depth and the amplitude measured can be used to calculate the effective stiffness value, measured as a function of frequency [87]. Analysis of the phase shift between the force and sample deformation enables calculation of the storage (elastic deformation) and loss (viscous deformation) moduli (refer to Figure 12B). Depending on the material's characteristics, these moduli can often be related to each other.

These kinds of microrheological measurements can now be conveniently carried out with commercially available software and cantilever packages, and enable the routine analysis of viscoelastic samples [88]. Figure 12C shows living fibroblasts measured in liquid. The corresponding storage and loss moduli mapped over the inset region can be seen in Figure 12D and Figure 12E.

Mapping and Microrheology Measurements on Large Area Tissue Samples

The dimensions and surface roughness of large biological and clinical samples often make an analysis in their native state challenging [52]. The standard 100 µm × 100 µm × 15 µm scan range of conventional AFM XYZ-scanners is often insufficient for achieving a statistically reliable characterization of samples with a diverse range of features. For this reason, innovative features, such as SmartMapping [56], have become indispensable for the large-scale nanomechanical characterization of tissues, thicker multi-cellular layers, and extracellular matrix and the cells residing within it.

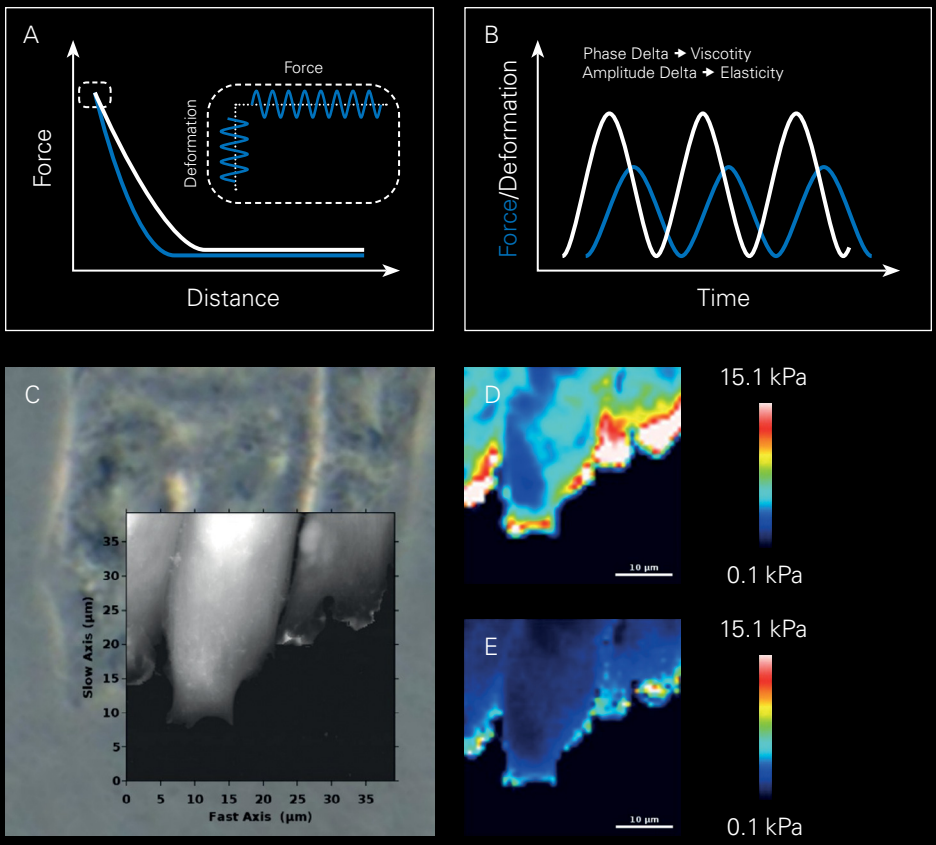

Figure 12

Microrheological measurements on living fibroblasts.

(A) Example of a characteristic FD curve performed on living cells. The difference between the approach and retraction segments is attributed to the viscous response of the material. The inset at the turn-around setpoint is the position where the sample is subjected to sinusoidal modulation and is part of the dynamic mechanical analysis.

(B) Frequency analysis of the phase shift between force and sample deformation enables the computational determination of the elastic and viscous response of the sample.

(C) Phase contrast image of living fibroblasts measured in cell culture medium at 37 °C. The inset shows the topography of the sample collected with QI mode.

(D) and (E) are the loss and storage moduli measured in the inset location in (C).

Figure 13A illustrates automated, large-range, mechanical measurements on a sheep muscle tissue sample over 110 µm in the Z direction. Measurement of the highly irregular, rough tissue surface was made possible using SmartMapping, which uses the integrated Z-motors to virtually overcome the limitations of the Z-piezo range of the BioAFM. The nanomechanical and optical characterization of the large sample area was possible by combining a motorized stage (XY-scan range of 20 mm × 20 mm) with optical tiling [89].

Figure 13B and C depict the frequency-dependent response of the sheep muscle tissue sample. The data were acquired by performing sinusoidal oscillations (at up to 250 Hz and an amplitude of 10 nm) in the Z direction while the probe was in contact with the sample surface. The viscoelastic properties of the samples were characterized using the distribution of the dynamic storage (E') and loss (E'') moduli, and their loss tangent relation ratio.

Correlative Microscopy Applications

As outlined above, a BioAFM can easily be combined with advanced optical and super-resolution microscopy techniques. Correlative measurements provide a unique perspective by combining topographical, three-dimensional, and mechanical atomic force microscopy data with the immunochemical identification of specific individual molecules and living cells from optical measurements. Bruker BioAFMs can be seamlessly integrated into optical microscopes, and commercially available calibration methods, such as the DirectOverlay feature, enable the perfect overlay of optical and atomic force microscopy data. Some of the primary advantages of correlative atomic force microscopy on living cells and tissues have already been demonstrated in Figure 11-13.

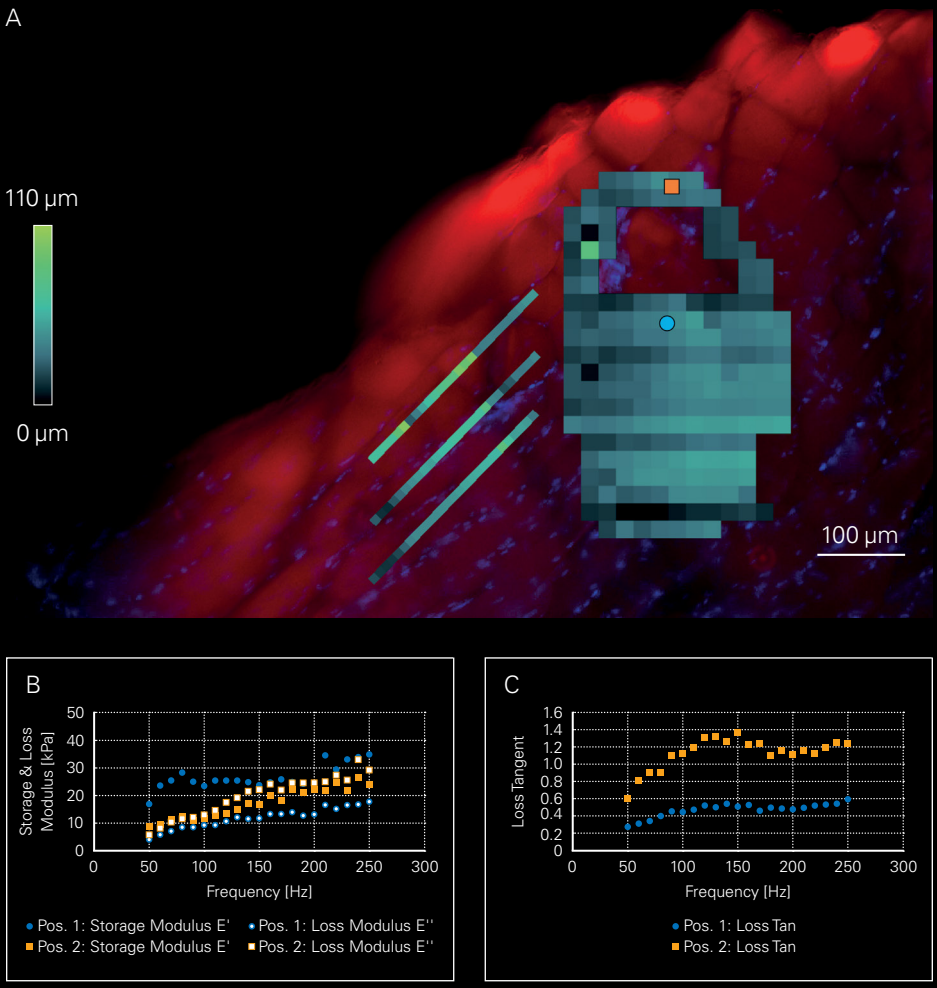

Figure 13

Force map of a cross-sectional slice of sheep muscle tissue.

(A) Force maps of user defined shapes on a cross-section of sheep muscle tissue overlayed with an optical fluorescence tiling image (scalebar 100 µm). Muscle fibers, rich in actin filaments, were stained with phalloidin-TRITC (red) and cell nuclei with DAPI (blue). Internal dark areas depict unlabeled connective tissue. Force maps were acquired in SmartMapping mode and illustrate the combined height measurement of samples with large topographies.

(B) Plot of storage and loss moduli recorded at different positions on the tissue.

(C) The calculated loss tangent ratio at the different measurement locations on the sample.

Recent advances in super-resolution methods have narrowed the resolution gap between atomic force microscopy and optical microscopy. Super-resolution techniques, including STED, STORM, SIM, and minimal photon fluxes (MINFLUX), now routinely deliver sub-diffraction resolution and precise localization capabilities. Specimens (e.g., DNA origami structures) are now readily available as calibration standards for 2D and 3D super-resolution optical microscopes [90-92]. Commercially available DNA-based rulers with a precision of a few nanometers allow the quantification and calibration of super-resolution systems and are available in various forms, fluorophore spacings, fluorescence tags, and nanostructured shapes and sizes [93].

Figure 14 shows correlative microscopy images of DNA nanostructures imaged by a BioAFM and STED microscopy combination [94]. The selected STED nanorulers [93] are rod-shaped and modified with dye molecules at finite distances along the rod (Figure 14A and Figure 14B). Following reduction of the effective spot size in the STED images, it is possible to evaluate the distance between individual fluorophores along selected nanorulers. The intensities along the arbitrarily drawn cross-sections were fit with a bi-sigmoidal Gaussian function (Figure 14C, D), resulting in peak-to-peak/center-to-center distances of 156 nm and 73 nm for the SIM 160R and STED 70R nanorulers. Such values are well within the 5 % confidence interval of the theoretical values of 160 and 70 nm.

Using the DirectOverlay feature to correlate and linearize the XY positions of the optical and AFM coordination systems enables the flexible selection of areas in the optical image and collection of atomic force microscopy images at even higher resolution (Figure 14G, H). The 200 nm length of the nanorulers measured in the atomic force microscopy images correlates well with previously reported values for similar structures [92]. The information from the optical and atomic force microscopy channels also correlates very well (Figure 14E, F).

.

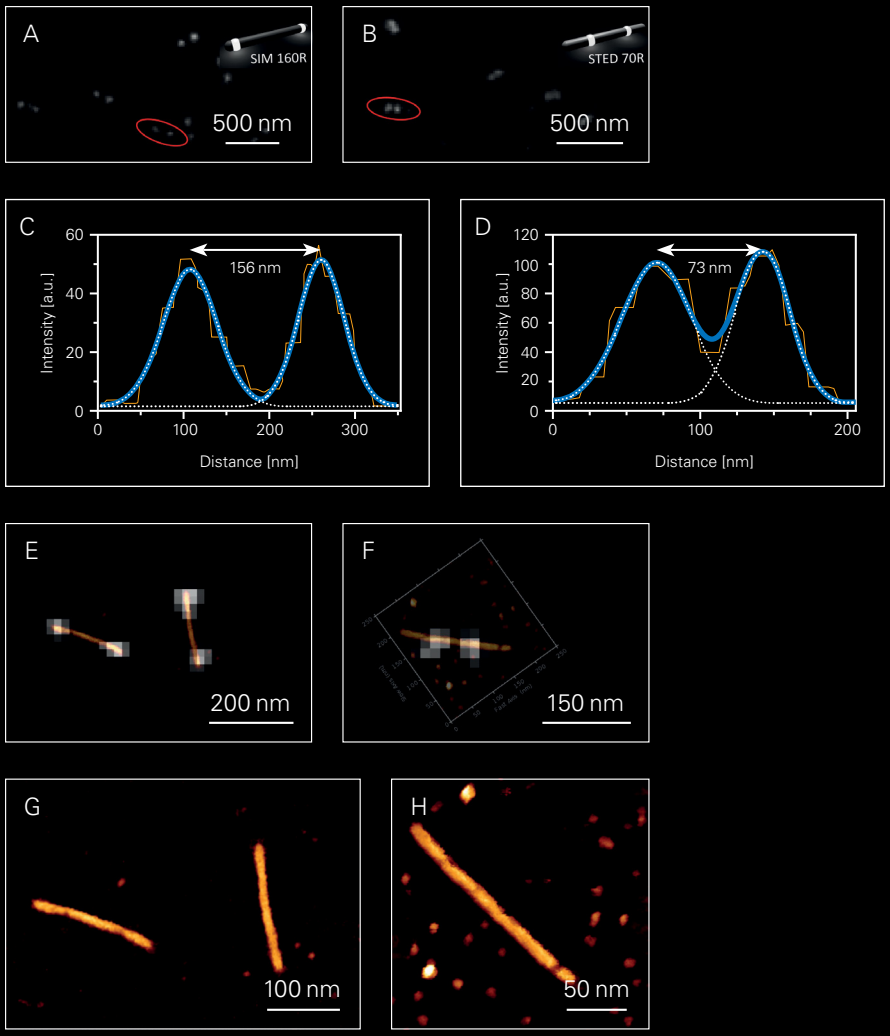

Figure 14

Correlative atomic force microscopy of DNA Nanorulers

(A, B) are STED measurements of the corresponding SIM 160R and STED 70R nanorulers, measured in TAE-1x (Mg) buffer. Insets are sketches of GATTAquant nanorulers with different mark-to-mark distances (70-160 nm, both labelled with Atto647N), reproduced with permission from [93]. (C, D) Bi-sigmoidal Gaussian fits of the intensity signal along the signified cross-sections in (A, B). (E, F) Optical correlation of the consecutively acquired STED and atomic force microscopy images of the DNA nanorulers. (G, H) QI topography channels of the AFM images used for the overlays in (E, F), showing the linearized structure of the DNA nanorulers (Z-scale: 10 nm).

Outlook and Future Trends

BioAFMs are now established, invaluable nanoanalytical tools in biological research and have numerous advantages over classical microscopy techniques. The ability to combine imaging, biomechanical analysis, and the study of dynamic mechanisms with high spatiotemporal resolution under near-physiological conditions has contributed to numerous fundamental breakthroughs in life science research.

BioAFMs have paved the way towards a more interdisciplinary approach in biomedical research and preclinical diagnostics. A host of innovative technological developments have resulted in the continuous expansion of the atomic force microscopy user base, and more recently from researchers working predominantly in engineering, biophysics, and physics to users in microscopy facilities and labs dedicated to molecular and cell biology, in both academic and industrial environments.

BioAFM has already become a key tool in fields such as biomedical research, bioengineering, and drug discovery [95], and the scope of possibilities and applications is limited only by the imagination.

The advances in high-speed instrumentation have firmly established atomic force microscopy as the high-resolution technique of choice for investigating dynamic molecular processes taking place on the sub-20 ms timescale and beyond [49]. By becoming a fully automated tool for the analysis of large tissue and biopsy samples, atomic force microscopy is expected to extend its firm foothold in biomedical research and preclinical diagnostics [55]. Furthermore, new machine-learning driven opportunities for the acquisition and analysis of atomic force microscopy data are expected to strongly influence the technology and its use in the foreseeable future.

Acknowledgements

The NRO samples in Figure 8B were kindly provided by GATTAquant DNA Nanotechnologies GmbH.

The DON samples in Figure 9 were imaged as a part of collaboration with Carmen M. Domínguez and Prof. Christof M. Niemeyer, Institute for Biological Interfaces (IBG-1), KIT, Germany.

The (GB1)8 sample in Figure 10 was provided courtesy of Prof. Yi Cao, Dept. of Physics, Nanjing University, China.

The NIH-3T3 murine fibroblasts in Figure 11 were provided by Stefanie Wedepohl, Freie Universität Berlin, Germany.

The sheep muscle tissue cross-sections in Figure 13 were provided courtesy of Prof. Ansgar Petersen, BIH, Center for Regenerative Therapies, Charité Medical University, Berlin, Germany.

References

[1] Hooke R (1665) Micrographia : or, Some physiological descriptions of minute bodies made by magnifying glasses. With observations and inquiries thereupon. London : Printed by J. Martyn and J. Allestry

[2] Leeuwenhoek AV (1674) More observations from Mr. Leewenhook, in a letter of Sept. 7. 1674. sent to the publisher, Philos Trans R Soc Lond 9 (108), 178-182.

[3] Van Zuylen J (1981) The microscopes of Antoni van Leeuwenhoek, J Microsc 121 (3), 309-328.

[4] Knoll M, Ruska E (1932) Das Elektronenmikroskop, Z Für Phys 78 (5–6), 318-339.

[5] Marton L (1934) La microscope électronique des objects biologique, Acud R Belg Bull Cl Sci 5 (20), 439-446.

[6] Driest E, Müller H-O (1935) Elektronenmikroskopische Aufnahmen (Elektronenmikrogramme) von Chitinobjekten, Z Für Wiss Mikrosk Für Mikrosk Tech 52 53-57.

[7] Krause F (1936) Elektronenoptische Aufnahmen von Diatomeen mit dem magnetischen Elektronenmikroskop, Z Für Phys 102 (5–6), 417-422.

[8] Krause F (1937) Das magnetische Elektronenmikroskop und seine Anwendung in der Biologie, Naturwissenschaften 25 (51), 817-825.

[9] Piontek MC, Roos WH (2018) Atomic Force Microscopy: An Introduction. In: Peterman EJG (ed) Single Molecule Analysis. Springer New York, New York, NY, pp 243-258

[10] Binnig G, Rohrer H, Gerber Ch, Weibel E (1982) Surface Studies by Scanning Tunneling Microscopy, Phys Rev Lett 49 (1), 57-61.

[11] Amrein M, Stasiak A, Gross H, Stoll E, Travaglini G (1988) Scanning Tunneling Microscopy of recA-DNA Complexes Coated with a Conducting Film, Science 240 (4851), 514-516.

[12] Baró AM, Miranda R, Alamán J, García N, Binnig G, Rohrer H, Gerber Ch, Carrascosa JL (1985) Determination of surface topography of biological specimens at high resolution by scanning tunnelling microscopy, Nature 315 (6016), 253-254.

[13] Binnig G, Quate CF, Gerber Ch (1986) Atomic Force Microscope, Phys Rev Lett 56 (9), 930-933.

[14] Marti O, Drake B, Hansma PK (1987) Atomic force microscopy of liquid-covered surfaces: Atomic resolution images, Appl Phys Lett 51 (7), 484-486.

[15] Drake B, Prater CB, Weisenhorn AL, Gould SAC, Albrecht TR, Quate CF, Cannell DS, Hansma HG, Hansma PK (1989) Imaging Crystals, Polymers, and Processes in Water with the Atomic Force Microscope, Science 243 (4898), 1586-1589.

[16] Barrett RC (1991) High-speed, large-scale imaging with the atomic force microscope, J Vac Sci Technol B Microelectron Nanometer Struct 9 (2), 302.

[17] Karrasch S, Hegerl R, Hoh JH, Baumeister W, Engel A (1994) Atomic force microscopy produces faithful high-resolution images of protein surfaces in an aqueous environment., Proc Natl Acad Sci 91 (3), 836-838.

[18] Rief M, Gautel M, Oesterhelt F, Fernandez JM, Gaub HE (1997) Reversible Unfolding of Individual Titin Immunoglobulin Domains by AFM, Science 276 (5315), 1109-1112.

[19] Benoit M, Gabriel D, Gerisch G, Gaub HE (2000) Discrete interactions in cell adhesion measured by single-molecule force spectroscopy, Nat Cell Biol 2 (6), 313-317.

[20] Pujals S, Feiner-Gracia N, Delcanale P, Voets I, Albertazzi L (2019) Super-resolution microscopy as a powerful tool to study complex synthetic materials, Nat Rev Chem 3 (2), 68-84.

[21] Liu S, Hoess P, Ries J (2022) Super-Resolution Microscopy for Structural Cell Biology, Annu Rev Biophys 51 (1), 301-326.

[22] De Jonge N, Ross FM (2011) Electron microscopy of specimens in liquid, Nat Nanotechnol 6 (11), 695-704.

[23] Ando T (2014) High-speed AFM imaging, Curr Opin Struct Biol 28 63-68.

[24] Amrein MW, Stamov D (2019) Atomic Force Microscopy in the Life Sciences. In: Hawkes PW, Spence JCH (eds) Springer Handbook of Microscopy. Springer International Publishing, Cham, pp 1469-1505

[25] Hooke R (1678) Lectures De Potentia Restitutiva, or of Spring, Explaining the Power of Springing Bodies. John Martyn, Printer to the Royal Society, London

[26] Dürig U (1999) Conservative and dissipative interactions in dynamic force microscopy, Surf Interface Anal 27 (5–6), 467-473.

[27] Krieg M, Fläschner G, Alsteens D, Gaub BM, Roos WH, Wuite GJL, Gaub HE, Gerber C, Dufrêne YF, Müller DJ (2019) Atomic force microscopy-based mechanobiology, Nat Rev Phys 1 (1), 41-57.

[28] Bruker Nano Surfaces PeakForce Tapping. In: AFM Types - PeakForce Tapping. https://www.bruker.com/en/products-and-solutions/microscopes/materials-afm/afm-modes/peakforce-tapping.html

[29] Bruker Nano Surfaces PeakForce QNM. In: AFM Types - PeakForce QNM. https://www.bruker.com/en/products-and-solutions/microscopes/materials-afm/afm-modes/peakforce-qnm.html

[30] Kodera N, Sakashita M, Ando T (2006) Dynamic proportional-integral-differential controller for high-speed atomic force microscopy, Rev Sci Instrum 77 (8), 083704.

[31] Ando T, Uchihashi T, Scheuring S (2014) Filming Biomolecular Processes by High-Speed Atomic Force Microscopy, Chem Rev 114 (6), 3120-3188.

[32] Heuberger M, Dietler G, Schlapbach L (1996) Elastic deformations of tip and sample during atomic force microscope measurements, J Vac Sci Technol B Microelectron Nanometer Struct Process Meas Phenom 14 (2), 1250-1254.

[33] JPK Instruments The new JPK Contact Point Imaging (CPI) option based on QI mode

[34] Stamov DR, Stock E, Franz CM, Jähnke T, Haschke H (2015) Imaging collagen type I fibrillogenesis with high spatiotemporal resolution, Ultramicroscopy 149 86-94.

[35] Owen RJ, Heyes CD, Knebel D, Röcker C, Nienhaus GU (2006) An integrated instrumental setup for the combination of atomic force microscopy with optical spectroscopy, Biopolymers 82 (4), 410-414.

[36] Gómez-Varela AI, Stamov DR, Miranda A, Alves R, Barata-Antunes C, Dambournet D, Drubin DG, Paiva S, De Beule PAA (2020) Simultaneous co-localized super-resolution fluorescence microscopy and atomic force microscopy: combined SIM and AFM platform for the life sciences, Sci Rep 10 (1), 1122.

[37] Hell SW, Wichmann J (1994) Breaking the diffraction resolution limit by stimulated emission: stimulated-emission-depletion fluorescence microscopy, Opt Lett 19 (11), 780.

[38] Odermatt PD, Shivanandan A, Deschout H, Jankele R, Nievergelt AP, Feletti L, Davidson MW, Radenovic A, Fantner GE (2015) High-Resolution Correlative Microscopy: Bridging the Gap between Single Molecule Localization Microscopy and Atomic Force Microscopy, Nano Lett 15 (8), 4896-4904.

[39] Balzarotti F, Eilers Y, Gwosch KC, Gynnå AH, Westphal V, Stefani FD, Elf J, Hell SW (2017) Nanometer resolution imaging and tracking of fluorescent molecules with minimal photon fluxes, Science 355 (6325), 606-612.

[40] Gwosch KC, Pape JK, Balzarotti F, Hoess P, Ellenberg J, Ries J, Hell SW (2020) MINFLUX nanoscopy delivers 3D multicolor nanometer resolution in cells, Nat Methods 17 (2), 217-224.

[41] Bruker Nano Surfaces DirectOverlay 2 Software Module. In: BioAFM Accessories Add- - DirectOverlay 2 Softw. Module. https://www.bruker.com/de/products-and-solutions/microscopes/bioafm/bioafm-accessories/directoverlay-2-software-module.html

[42] Jähnke T, Haggerty M (2008) Method for the operation of a measurement system with a scanning probe microscope, and measurement system

[43] Harke B, Chacko JV, Haschke H, Canale C, Diaspro A (2012) A novel nanoscopic tool by combining AFM with STED microscopy, Opt Nanoscopy 1 (1), 3.

[44] Miranda A, Gómez-Varela AI, Stylianou A, Hirvonen LM, Sánchez H, De Beule PAA (2021) How did correlative atomic force microscopy and super-resolution microscopy evolve in the quest for unravelling enigmas in biology?, Nanoscale 13 (4), 2082-2099.

[45] Viani MB, Pietrasanta LI, Thompson JB, Chand A, Gebeshuber IC, Kindt JH, Richter M, Hansma HG, Hansma PK (2000) Probing protein–protein interactions in real time, Nat Struct Biol 7 (8), 644-647.

[46] Ando T, Kodera N, Takai E, Maruyama D, Saito K, Toda A (2001) A high-speed atomic force microscope for studying biological macromolecules, Proc Natl Acad Sci 98 (22), 12468-12472.

[47] Picco LM, Bozec L, Ulcinas A, Engledew DJ, Antognozzi M, Horton MA, Miles MJ (2007) Breaking the speed limit with atomic force microscopy, Nanotechnology 18 (4), 044030.

[48] Ando T (2012) High-speed atomic force microscopy coming of age, Nanotechnology 23 (6), 062001.

[49] Stamov DR, Neumann T, Kraus A, Körnig A, Jankowski T, Knebel D, Jähnke T, Henze T, Haschke H (2022) Unraveling Molecular Dynamics with High-Speed Video-Rate Atomic Force Microscopy, Microsc Today 30 (3), 10-14.

[50] Bruker Nano Surfaces (2019) High-speed imaging of DNA submolecular structure and dynamics. Microsc. Anal.

[51] Monserrate A, Casado S, Flors C (2014) Correlative Atomic Force Microscopy and Localization-Based Super-Resolution Microscopy: Revealing Labelling and Image Reconstruction Artefacts, ChemPhysChem 15 (4), 647-650.

[52] Fuhs T, Wetzel F, Fritsch AW, Li X, Stange R, Pawlizak S, Kießling TR, Morawetz E, Grosser S, Sauer F, Lippoldt J, Renner F, Friebe S, Zink M, Bendrat K, Braun J, Oktay MH, Condeelis J, Briest S, Wolf B, Horn L-C, Höckel M, Aktas B, Marchetti MC, Manning ML, Niendorf A, Bi D, Käs JA (2022) Rigid tumours contain soft cancer cells, Nat Phys 18 (12), 1510-1519.

[53] Bruker Nano Surfaces HybridStage. In: BioAFM Accessories Add-- HybridStage. https://www.bruker.com/en/products-and-solutions/microscopes/bioafm/bioafm-accessories/hybridstage.html

[54] Käs JA, Fuhs T, Müller T, Körnig A (2019) Mapping large areas of life science samples. Wiley Anal. Sci.

[55] Tschaikowsky M, Neumann T, Brander S, Haschke H, Rolauffs B, Balzer BN, Hugel T (2021) Hybrid fluorescence-AFM explores articular surface degeneration in early osteoarthritis across length scales, Acta Biomater S1742706121001823.

[56] Bruker Nano Surfaces SmartMapping. In: AFM Modes - SmartMapping. https://www.bruker.com/en/products-and-solutions/microscopes/bioafm/bioafm-modes/smartmapping.html

[57] Sulchek T, Minne SC, Adams JD, Fletcher DA, Atalar A, Quate CF, Adderton DM (1999) Dual integrated actuators for extended range high speed atomic force microscopy, Appl Phys Lett 75 (11), 1637-1639.

[58] El Rifai K, El Rifai O, Youcef-Toumi K (2004) On dual actuation in atomic force microscopes. In: Proceedings of the 2004 American Control Conference. IEEE, Boston, MA, USA, pp 3128-3133 vol.4

[59] Knebel D, Amrein M, Voigt K, Reichelt R (1997) A fast and versatile scan unit for scanning probe microscopy: A fast and versatile scan unit for SPM, Scanning 19 (4), 264-268.

[60] Egawa, Chiba, Homma, Chinone, Muramatsu (1999) High-speed scanning by dual feedback control in SNOM/AFM, J Microsc 194 (2-3), 325-328.

[61] Jeong Y, Jayanth GR, Menq C-H (2007) Control of tip-to-sample distance in atomic force microscopy: A dual-actuator tip-motion control scheme, Rev Sci Instrum 78 (9), 093706.

[62] Kuiper S, Fleming AJ, Schitter G (2010) Dual Actuation for High Speed Atomic Force Microscopy, IFAC Proc Vol 43 (18), 220-226.

[63] Nievergelt AP, Erickson BW, Hosseini N, Adams JD, Fantner GE (2015) Studying biological membranes with extended range high-speed atomic force microscopy, Sci Rep 5 (1), 11987.

[64] Haggerty M (2008) DEVICE AND METHOD FOR A PROBE MICROSCOPIC EXAMINATION OF A SAMPLE

[65] Bruker Nano Surfaces CellHesion 300. In: At. Force Microsc. - CellHesion 300. https://www.bruker.com/en/products-and-solutions/microscopes/bioafm/jpk-cellhesion.html

[66] Rothemund PWK (2006) Folding DNA to create nanoscale shapes and patterns, Nature 440 (7082), 297-302.

[67] Keller A, Linko V (2020) Challenges and Perspectives of DNA Nanostructures in Biomedicine, Angew Chem Int Ed 59 (37), 15818-15833.

[68] Douglas SM, Dietz H, Liedl T, Högberg B, Graf F, Shih WM (2009) Self-assembly of DNA into nanoscale three-dimensional shapes, Nature 459 (7245), 414-418.

[69] Dey S, Fan C, Gothelf KV, Li J, Lin C, Liu L, Liu N, Nijenhuis MAD, Saccà B, Simmel FC, Yan H, Zhan P (2021) DNA origami, Nat Rev Methods Primer 1 (1), 13.

[70] Rothemund PWK (2005) Design of DNA origami. In: ICCAD-2005. IEEE/ACM International Conference on Computer-Aided Design, 2005. IEEE, San Jose, CA, pp 471-478

[71] Douglas SM, Marblestone AH, Teerapittayanon S, Vazquez A, Church GM, Shih WM (2009) Rapid prototyping of 3D DNA-origami shapes with caDNAno, Nucleic Acids Res 37 (15), 5001-5006.

[72] Bruker Nano Surfaces (2021) True High-Speed AFM Visualization of DNA Origami Molecular Dynamics at 50 frames/sec. Microsc. Anal.

[73] Hu Y, Domínguez CM, Christ S, Niemeyer CM (2020) Postsynthetic Functionalization of DNA-Nanocomposites with Proteins Yields Bioinstructive Matrices for Cell Culture Applications, Angew Chem Int Ed 59 (43), 19016-19020.

[74] Lanzerstorfer P, Müller U, Gordiyenko K, Weghuber J, Niemeyer CM (2020) Highly Modular Protein Micropatterning Sheds Light on the Role of Clathrin-Mediated Endocytosis for the Quantitative Analysis of Protein-Protein Interactions in Live Cells, Biomolecules 10 (4), 540.

[75] Zlatanova J, Lindsay SM, Leuba SH (2000) Single molecule force spectroscopy in biology using the atomic force microscope, Prog Biophys Mol Biol 74 (1–2), 37-61.

[76] Scholl ZN, Marszalek PE (2018) AFM-Based Single-Molecule Force Spectroscopy of Proteins. In: Lyubchenko YL (ed) Nanoscale Imaging. Springer New York, New York, NY, pp 35-47

[77] Ott W, Jobst MA, Bauer MS, Durner E, Milles LF, Nash MA, Gaub HE (2017) Elastin-like Polypeptide Linkers for Single-Molecule Force Spectroscopy, ACS Nano 11 (6), 6346-6354.

[78] Carrion-Vazquez M, Oberhauser AF, Fowler SB, Marszalek PE, Broedel SE, Clarke J, Fernandez JM (1999) Mechanical and chemical unfolding of a single protein: A comparison, Proc Natl Acad Sci 96 (7), 3694-3699.

[79] Cao Y, Li H (2007) Polyprotein of GB1 is an ideal artificial elastomeric protein, Nat Mater 6 (2), 109-114.

[80] Jerry Qi H, Ortiz C, Boyce MC (2006) Mechanics of Biomacromolecular Networks Containing Folded Domains, J Eng Mater Technol 128 (4), 509-518.

[81] Meyer AC, Öz Y, Gundlach N, Karbach M, Lu P, Müller G (2020) Molecular chains under tension: Thermal and mechanical activation of statistically interacting extension and contraction particles, Phys Rev E 101 (2), 022504.

[82] Kollmannsberger P, Fabry B (2011) Linear and Nonlinear Rheology of Living Cells, Annu Rev Mater Res 41 (1), 75-97.

[83] Alcaraz J, Buscemi L, Grabulosa M, Trepat X, Fabry B, Farré R, Navajas D (2003) Microrheology of Human Lung Epithelial Cells Measured by Atomic Force Microscopy, Biophys J 84 (3), 2071-2079.

[84] Moeendarbary E, Valon L, Fritzsche M, Harris AR, Moulding DA, Thrasher AJ, Stride E, Mahadevan L, Charras GT (2013) The cytoplasm of living cells behaves as a poroelastic material, Nat Mater 12 (3), 253-261.

[85] Rother J, Nöding H, Mey I, Janshoff A (2014) Atomic force microscopy-based microrheology reveals significant differences in the viscoelastic response between malign and benign cell lines, Open Biol 4 (5), 140046.

[86] Abuhattum S, Mokbel D, Müller P, Soteriou D, Guck J, Aland S (2022) An explicit model to extract viscoelastic properties of cells from AFM force-indentation curves, iScience 25 (4), 104016.

[87] Abuhattum S, Körnig A (2023) Microrheological Measurements on Soft Materials with Atomic Force Microscopy. Bruker Nano Surfaces

[88] Bruker Nano Surfaces (2020) CellMech Package

[89] Bruker Nano Surfaces DirectTiling Software Module. In: BioAFM Accessories Add- - DirectTiling Softw. Module. https://www.bruker.com/en/products-and-solutions/microscopes/bioafm/bioafm-accessories/directtiling-software-module.html

[90] Steinhauer C, Jungmann R, Sobey TL, Simmel FC, Tinnefeld P (2009) DNA Origami as a Nanoscopic Ruler for Super-Resolution Microscopy, Angew Chem Int Ed 48 (47), 8870-8873.

[91] Schmied JJ, Forthmann C, Pibiri E, Lalkens B, Nickels P, Liedl T, Tinnefeld P (2013) DNA Origami Nanopillars as Standards for Three-Dimensional Superresolution Microscopy, Nano Lett 13 (2), 781-785.

[92] Schmied JJ, Raab M, Forthmann C, Pibiri E, Wünsch B, Dammeyer T, Tinnefeld P (2014) DNA origami–based standards for quantitative fluorescence microscopy, Nat Protoc 9 (6), 1367-1391.

[93] Gattaquant DNA Nanotechnologies Gattaquant DNA Nanotechnologies. https://www.gattaquant.com/

[94] Neuman T, Barner J, Stamov D (2019) Correlative AFM and Super-Resolution STED Analysis of DNA Nanostructures

[95] Liang W, Shi H, Yang X, Wang J, Yang W, Zhang H, Liu L (2020) Recent advances in AFM-based biological characterization and applications at multiple levels, Soft Matter 16 (39), 8962-8984.

Further Resources

Bruker's AFM Solutions for Life Sciences Research:
https://www.bruker.com/bioafm

BioAFM Accessories:
https://www.bruker.com/en/products-and-solutions/microscopes/bioafm/bioafm-accessories.html

Suscribe to our Journal Club to Keep Up to Date on the Latest in BioAFM Research:
https://www.bruker.com/en/products-and-solutions/microscopes/bioafm/bioafm-journal-club.html

JPK BioAFM Business
Nano Surfaces and Metrology Division
Bruker Nano GmbH

Am Studio 2D · 12489 Berlin, Germany
tel.: +49 30 670990 7500 · fax: +49 30 670990 30

www.bruker.com/bioafm

Contact us!